

AD A116664

RADC-TR-82-73
Final Technical Report
April 1982



ADAPTIVE NONLINEAR CANCELLER (ANLC)

General Atronic Corporation

Lawrence R. Burgess and David M. Cooper

APPROVED FOR PUBLIC RELEASE; DISTRIBUTION UNLIMITED

DTIC
S JUL 7 1982
A

ROME AIR DEVELOPMENT CENTER
Air Force Systems Command
Griffiss Air Force Base, NY 13441

DTIC FILE COPY

82 07 07 029

This report has been reviewed by the RADC Public Affairs Office (PA) and is releasable to the National Technical Information Service (NTIS). At NTIS it will be releasable to the general public, including foreign nations.

RADC-TR-82-73 has been reviewed and is approved for publication.

APPROVED: *Wayne E. Woodward*

WAYNE E. WOODWARD
Project Engineer

APPROVED: *David C. Luke*

DAVID C. LUKE, Colonel, USAF
Chief, Reliability & Compatibility Division

FOR THE COMMANDER: *John P. Huss*

JOHN P. HUSS
Acting Chief, Plans Office

If your address has changed or if you wish to be removed from the RADC mailing list, or if the addressee is no longer employed by your organization, please notify RADC.(RBCT) Griffiss AFB NY 13441. This will assist us in maintaining a current mailing list.

Do not return copies of this report unless contractual obligations or notices on a specific document requires that it be returned.

UNCLASSIFIED

SECURITY CLASSIFICATION OF THIS PAGE (When Data Entered)

REPORT DOCUMENTATION PAGE		READ INSTRUCTIONS BEFORE COMPLETING FORM
1. REPORT NUMBER RADC-TR-82-73	2. GOVT ACCESSION NO. /	3. RECIPIENT'S CATALOG NUMBER
4. TITLE (and Subtitle) ADAPTIVE NONLINEAR CANCELLER (ANLC)		5. TYPE OF REPORT & PERIOD COVERED Final Technical Report 1 Jun 80 - 1 Nov 81
		6. PERFORMING ORG. REPORT NUMBER N/A
7. AUTHOR(s) Lawrence R. Burgess David M. Cooper		8. CONTRACT OR GRANT NUMBER(s) F30602-80-C-0202
9. PERFORMING ORGANIZATION NAME AND ADDRESS General Atronics Corp. (Magnavox) 1200 East Mermaid Lane Philadelphia PA 19118		10. PROGRAM ELEMENT, PROJECT, TASK AREA & WORK UNIT NUMBERS 62702F 23380413
11. CONTROLLING OFFICE NAME AND ADDRESS Rome Air Development Center (RBCT) Griffiss AFB NY 13441		12. REPORT DATE April 1982
		13. NUMBER OF PAGES 63
14. MONITORING AGENCY NAME & ADDRESS (if different from Controlling Office) Same		15. SECURITY CLASS. (of this report) UNCLASSIFIED
		15a. DECLASSIFICATION/DOWNGRADING SCHEDULE N/A
16. DISTRIBUTION STATEMENT (of this Report) Approved for public release; distribution unlimited.		
17. DISTRIBUTION STATEMENT (of the abstract entered in Block 20, if different from Report) Same		
18. SUPPLEMENTARY NOTES RADC Project Engineer: Wayne E. Woodward (RBCT)		
19. KEY WORDS (Continue on reverse side if necessary and identify by block number) Electromagnetic Compatibility Intermodulation Interference Cancellation		
20. ABSTRACT (Continue on reverse side if necessary and identify by block number) This study was directed at the analysis and characterization of non-linearities associated with the AFSATCOM/ALT-32H interference problem and the development of an automatic nonlinear cancellation system. Analysis included the use of power series, Volterra series, and perturbation analysis to predict the generation of intermodulation products. Characterization studies included the use of variable power input two-tone or notch noise to measure IMP generation by various nonlinear devices.		

DD FORM 1473 1 JAN 73 EDITION OF 1 NOV 65 IS OBSOLETE

UNCLASSIFIED

SECURITY CLASSIFICATION OF THIS PAGE (When Data Entered)

UNCLASSIFIED

SECURITY CLASSIFICATION OF THIS PAGE(When Data Entered)

Manual and automatic nonlinear interference cancellation systems were designed and implemented.

Experimental studies were conducted using different nonlinearities, a wide range of input powers, a wide range of frequency spectra exciting the nonlinearities, various delays and multipath before and after the nonlinearities, and a number of modulation formats. Based on these experimental studies, a list of necessary conditions for nonlinear cancellation were developed. To achieve a good automatic nonlinear cancellation, the following conditions must be met:

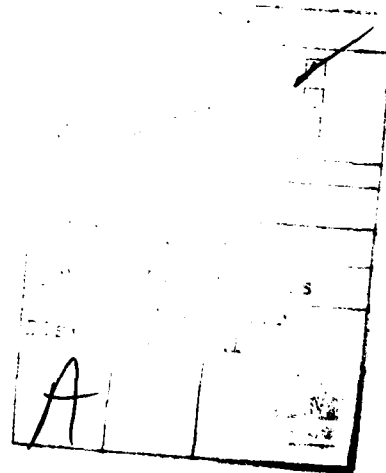
- (1) A good nonlinear reference must be generated.
- (2) Amplitude versus frequency shape of the signal impinging on the interfering and reference nonlinearities are critically important for good nonlinear cancellation.
- (3) Interfering and reference nonlinearity types must be matched.
- (4) Multipath before the interfering and reference nonlinearities is critically important. A multipath difference on the order of a few feet will cause complete loss of cancellation.
- (5) The total power input to the reference nonlinearity must be similar to that of the interfering nonlinearity for good cancellation.

UNCLASSIFIED

SECURITY CLASSIFICATION OF THIS PAGE(When Data Entered)

Table of Contents

1.0 INTRODUCTION..... 1
 1.1 Background.... 2
 1.2 Approach to Problem..... 4
 2.0 ANALYSIS..... 7
 2.1 Power Series Analysis of a Semiconductor Diode..... 7
 2.2 Perturbation and Volterra Analyses of Nonlinear Systems. 8
 3.0 CHARACTERIZATION STUDIES OF NONLINEARITIES..... 17
 3.1 Two-Tone Measurements of the Third-Order Intercept
 as a Function of Input Power..... 17
 3.2 Notched Noise Measurements of Intermodulation
 Distortion..... 19
 3.3 Effect of Diode Bias on Intermodulation Generation..... 23
 4.0 NONLINEAR CANCELLATION SYSTEMS..... 29
 4.1 Manual Cancellation..... 29
 4.2 Experimental Results for Manual Nonlinear Interference
 Cancellation..... 31
 4.3 Automatic Nonlinear Cancellation..... 39
 5.0 CONCLUSIONS..... 57
 5.1 Recommendations..... 58
 APPENDIX A - Noise Through a Third-Order Nonlinearity..... 61
 References..... 63



1.0 INTRODUCTION

The ever-increasing use of communication equipment aboard airborne platforms is creating a critical electromagnetic compatibility problem. The replacement of older equipment with new equipment utilizing solid state components, electromagnetically tuned filters, and wide band coverage is compounding the situation. Higher transmit powers and new transmission waveforms, especially spread spectrum types, add to the problem. The management of interference is especially important in satellite-based communication systems operating at low receive power densities with little margin.

Interference is either linear or nonlinear in origin. Linear interference results when a fundamental signal from a transmitter couples into a receiver and prevents detection or demodulation of the desired signal with the required fidelity or sensitivity. Nonlinear interference problems are those where the interference coupled into the receiver is a harmonic of one transmitter or some intermodulation product of two or more transmitted signals. The nonlinear interference is produced by one or more narrowband transmissions or a broadband noise transmission impinging on a nonlinearity. Sources of nonlinearities can be distributed over the airframe, or more often, in communication and navigation equipment.

The linear interference problem can be solved by a variety of techniques. Standard filtering approaches are by far the most widely used means of eliminating this form of interference. In addition, active interference cancellation techniques can be applied to solve those linear interference problems which cannot be solved by the application of spectral filtering. While not as mature as spectral filtering, linear interference techniques are well-known and the technology is available to solve many problems. Current activity in linear interference cancelling system technology is concerned with cancelling higher power interference, with broader bandwidths, faster response, less complexity, etc.

Currently available techniques of solving nonlinear interference problems are limited to spectrum management and the elimination of the interference-producing nonlinearities. Both of these approaches are becoming increasingly difficult to apply because of the demand for more communication channels and the wider bandwidth of the channels as well as the trend towards broader band, electronically-tuned communications equipment which frequently is a source of the nonlinearity. In order to provide an alternate technique for combatting nonlinear interference, the application of active cancellation concepts to nonlinear interference problems is being studied and implemented.

This report documents the results of a study of the nature of nonlinear interference from the standpoint of developing a working experimental model to automatically cancel nonlinearly generated interference. The study included a literature search of related material, analytic work, experimental measurements to characterize nonlinearities,

and implementation and evaluation of a variety of nonlinear interference cancellation systems.

A method to provide automatic nonlinear cancellation of intermodulation products generated by broadband noise impinging on a nonlinearity has been developed and implemented. This approach utilizes standard linear cancellation techniques in conjunction with a nonlinear reference generation techniques. Modification of the reference nonlinear transfer was used to match more closely the interfering transfer function so that better nonlinear cancellation could be obtained.

1.1 BACKGROUND

The identification, evaluation and elimination of nonlinearities on board Air Force aircraft is addressed in detail in reference [1]. As described in [1], a series of measurements were made on several aircraft. The measurements indicated that the predominant harmonic interferences were not produced by airframe effects ("rusty bolts," mechanical joints, etc.) as initially expected, but by nonlinearities in the communication and navigation system.

Further tests and measurements located some of the most troublesome causes of these nonlinearities and the relative magnitude of the distortion produced by these sources. Equipment modifications to reduce the production of distortion products were investigated, implemented, and evaluated.

Subsequent measurements of the SATCOM receivers have indicated that additional nonlinearities are present which produce distortion products falling in the satellite downlink band, thereby limiting the sensitivity of the receiver. This loss of sensitivity is particularly critical for satellite links such as AFSATCOM or the Global Positioning System (NAVSTAR) because these links usually operate with little margin. Aircraft on which distortion product interference is causing problems are the EC-135C RC-135, FB-111A, and B-52. References [2], [3], and [4] contain descriptions of other studies which analyzed nonlinearities and

[1] "Nonlinear Interference Cancellation System," RADC-TR-78-225, November 1978.

[2] Higa, Walter H., "Spurious Signals Generated by Electron Tunneling on Large Reflector Antennas," Proc IEEE, vol. 63, no. 2, February 1975.

[3] Chase, W.M., J.W. Rockway and G.C. Salisbury, "A Method of Detecting Significant Sources of Intermodulation Interference," IEEE Trans on Electromagnetic Compatibility, vol. EMC-17, no. 2, May 1975.

[4] Chase, W.M., "Ship RFI Survey Procedure for HF Frequencies," NELC Technical Document 336, 21 June 1974.

means of locating them on structures as large and complicated as Navy ships.

References [5], [6] and [7] document recent studies of intermodulation generation by nonlinear conduction mechanisms in normally passive hardware components.

The general problem of analysis of nonlinear effects has been addressed by researchers in various fields for many years. The early work of Wiener as well as the later work [8] represents some of the earliest efforts to apply the tools of mathematical analysis to the solution of nonlinear problems in engineering. Much of the analysis can be divided into consideration of two basic types of nonlinear systems: those with no memory and those containing memory. Memoryless systems (both linear and nonlinear) have the property that the system output at each instant of time is determined by the input at that instant and is unaffected by the past inputs to the system.

Much of the earlier applied work was restricted to the analysis of memoryless types of nonlinearities. More recent efforts have extended the earlier work to include nonlinearities with memory. Analysis of these more complicated nonlinearities requires more powerful analytical tools. There has been renewed interest in the solution of these problems by application of Volterra functional series. References [9], [10], and [11]

[5] Bond, C.D., Guenzer, C.S., "Intermodulation Generation by Electron Tunneling Through Aluminum-Oxide Film," Proc IEEE, Vol. 67, No. 12, December 1979.

[6] Arazm, F., Benson, F.A., "Nonlinearities in Metal Contacts at Microwave Frequencies," IEEE Trans on Electromagnetic Compatibility, vol. EMC-22, no. 3, August 1980.

[7] Lee, J.C., "Intermodulation Measurement in the UHF Band and an Analysis of Some Basic Materials," Lincoln Laboratory Technical Note 1979.

[8] Wiener, N. Nonlinear Problems in Random Theory, MIT Press, 1958.

[9] "Nonlinearity System Modelling and Analysis with Application to Communication,

[10] Spina, J.E., Weiner, D.D., Sinusoidal Analysis of Weakly Nonlinear Circuits, Van Nostrand Reinhold Co., 1980.

[11] Schetzen, M., The Volterra and Wiener Theories of Nonlinear Systems, John Wiley and Sons, New York, 1980.

[12] Colemeier, J., "Air Force Electromagnetic Compatibility Intrasystem Analysis Program," RADC, 1980.

contain a description of this series and its application to nonlinear analysis and is typical of current applications of Volterra analysis. Recently, programs have been developed to determine nonlinear transfer functions of electronic circuits using the Volterra Series approach. They are directed to such phenomena as intermodulation, cross-modulation, desensitization, gain compression/expansion, and AM-PM conversion, [12]

Most work reported to date involves the analysis of the distortion characteristics of devices and the computation of the levels of distortion products (DP) produced by these devices or the exact fundamental waveforms in the nonlinearity. Often, the analysis of the distortion characteristics of these devices is conducted for CW signals and, therefore, is not directly applicable to the problem of a more complex modulated carrier or noise input.

Much work has been done in the area of modelling and analysis of nonlinearities in semiconductor devices. References [13], [14] and [15] investigate intermodulation generated in semiconductor single diodes and transistors. Reference [16] represents an extension to include the effect of semiconductors on IMP generation in communication devices.

Some work is underway to provide equalization for the nonlinear characteristics of telephone channels. Reference [17] reports on the application of these techniques to baseband equalization of telephone line nonlinearities. To date, no work has been reported on successful adaptive nonlinear cancellation of IMPs resulting from a noise input.

1.2 APPROACH TO PROBLEM

The objective of this effort was to investigate adaptive nonlinear cancellation techniques, culminating in an experimental model, that would lead to a solution of IMP problems associated with high power HF and UHF. Initially, a literature search was made of the work in the

[13] Gretsich, W R., "The Spectrum of Intermodulation Generated in a Semiconductor Diode Junction," Proc IEEE, vol. 54, no. 11, November 1966.

[14] Lotsch, H.K., "Theory of Nonlinear Distortion Produced in a Semiconductor Diode," IEEE Trans on Electron Devices, vol. ED-15, no. 5, May 1968.

[15] Bava, E., et al, "Analysis of Varactor Frequency Multiplexers: Nonlinear Behavior and Hysteresis Phenomena," IEEE Trans on Military Technology, vol. 27, no. 2, February 1979.

[16] "Intermodulation in Antenna Amplifiers," Amperex Application Report S-141, 1980.

[17] Falconer D.D., "Adaptive Equalization of Channel Nonlinearities in QAM Data Transmission Systems," BSTJ, vol. 57, no. 7, September 1978.

following areas: intermodulation formation in semiconductor devices and passive components; analysis of nonlinear systems using power series, Volterra series, perturbation theory, and Wiener theory, and studies that attempted to locate nonlinearities in communication systems. A good deal of effort was expended on the characterization of nonlinearities. Simple nonlinearities such as a FH1100 Schottky diode and a Motorola MWA 110 amplifier were characterized using twotones, narrowband noise, or broadband notch noise inputs. Attention was directed to the ability to match nonlinear transfer functions since, in most systems, a nonlinear reference is not available.

Analyses of simple nonlinear systems were made using power series, Volterra series, and a perturbation analysis. Results of each analysis were compared. Operational methods were developed which generated the same solution as analytical techniques.

Various nonlinear interference cancellation schemes were investigated. The underlying problem in all adaptive nonlinear canceller configurations is obtaining a nonlinear reference whose nonlinear component is larger than its linear component. Two schemes were implemented that would generate a good nonlinear reference, and automatically cancel nonlinear interference.

2.0 ANALYSIS

In this section, the harmonic signals and intermodulation products generated when one or more tones are incident on a nonlinearity are analytically investigated. In addition, the correspondence between third-order distortion products generated by a two-tone input and those generated by bandlimited noise is examined. Initially, the analysis assumes that the nonlinearities are memoryless, continuous and single-valued. Later distortion products generated by nonlinearities having memory are examined. Operational methods are developed that can generate solutions identical to those obtained using analytical techniques.

2.1 POWER SERIES ANALYSIS OF A SEMICONDUCTOR DIODE

A power series approach can be used to model a continuous, single-valued and memoryless nonlinearity. Since biased FH100 Schottky diodes were used as a source of a nonlinearity in much of our experimental work, a power series analysis was performed on such a device.

For frequencies well below the cutoff frequency of the semiconductor diode, the transfer characteristic is given by the exponential function:

$$I(V) = i_0 [e^{\alpha V(t)} - 1] = I_d + i = i_0 [e^{\alpha V_0} e^{\alpha v} - 1] \quad (2.1)$$

where $\alpha = \frac{8}{nkT} = \frac{1}{N} \frac{1}{26mV} 300^\circ K$, N is a constant ranging from 1 to 2 for germanium and 2 to 4 for silicon, I_d is the dc bias current, i is the incremental current, V_0 is the forward bias, v is the incremental voltage, and i_0 is the reverse saturation current.

Expanding $I(V)$ in a Taylor series expansion of the form

$$I(V) = \sum_{n=0}^{\infty} \frac{1}{n!} \frac{d^n I}{dV^n}(V_0) (V-V_0)^n$$

dropping the bias current term, letting $V-V_0 = v$, and truncating the series after a small number of terms results in an expression relating the incremental current to the incremental voltage.

$$i(v) = I_c \left[\frac{1}{26N} v + \frac{1}{2!} \left(\frac{1}{26N} \right)^2 v^2 + \frac{1}{3!} \left(\frac{1}{26N} \right)^3 v^3 + \dots \right]$$

where $I_c = i_0 e^{\alpha V_0}$. Note that if the linear term is considered, the bias current dependent series resistance is:

$$r = \frac{v}{i} = \frac{26N(mV)}{I_c(mA)}$$

PRECEDING PAGE BLANK-NOT FILMED

Setting the voltage across the diode to be $v = v_1 \cos \omega_1 t + v_2 \cos \omega_2 t$, and expanding up to third-order terms and using trigonometric identities results in:

$$\begin{aligned}
 i(t) \approx & \text{dc terms} + I_c \left[v_1 \left(\frac{1}{26N} \right) + \frac{1}{4} v_1 \left(\frac{1}{26N} \right)^3 \left(\frac{1}{2} v_1^2 + v_2^2 \right) \right] \cos \omega_1 t \\
 & + I_c \left[v_2 \left(\frac{1}{26N} \right) + \frac{1}{4} v_2 \left(\frac{1}{26N} \right)^3 \left(\frac{1}{2} v_2^2 + v_1^2 \right) \right] \cos \omega_2 t \\
 & + \frac{I_c}{4} \left(\frac{1}{26N} \right)^2 \left[v_1^2 \cos 2\omega_1 t + v_2^2 \cos 2\omega_2 t \right] + \frac{I_c}{24} \left(\frac{1}{26N} \right)^3 \left[v_1^3 \cos 3\omega_1 t + v_2^3 \cos 3\omega_2 t \right] \\
 & + \frac{I_c}{2} \left(\frac{1}{26N} \right)^2 \left[v_1 v_2 \cos(\omega_1 \pm \omega_2) t \right] + \frac{I_c}{2} \left(\frac{1}{26N} \right)^3 \left[v_1^2 v_2 \cos(2\omega_1 \pm \omega_2) t \right. \\
 & \left. + v_1 v_2^2 \cos(2\omega_2 \pm \omega_1) t \right]
 \end{aligned}$$

Note that for equal amplitude input tones ($v_1 = v_2$), the third-order intermodulation products are symmetric.

2.2 PERTURBATION AND VOLTERRA ANALYSES OF NONLINEAR SYSTEMS

In Section 2.1, a power series approach was used in the analysis of the memoryless nonlinear resistance of a diode. Using this type of analysis, nonlinear amplitude, but not nonlinear phase information, can be represented. In cases where phase distortion such as AM-to-PM conversion is of concern, other analysis techniques must be utilized. Both perturbation analysis and Volterra series are useful in analyzing frequency-dependent distortion.

One analytical method widely used in nonlinear analysis is the perturbation method. This method is applicable to equations where a small parameter is associated with the nonlinear terms. An approximate solution is found as a power series, with terms of the series involving the small parameter raised to successively higher powers. This technique was applied to a capacitance across a third-order nonlinear resistance in order to better understand the behavior of a diode-like device with memory (Figure 2.1).

Let the nonlinear incremental current behavior be described by:

$$i_{NL} = av + bv^3$$

The systems that were analyzed are shown in Figures 1a,b,c. In all cases, a diode-type nonlinearity was used with a two-tone input. Using Kirchoff's current law, the differential equation for Figure 4.1a is:

$$C \frac{dv}{dt} + av + bv^3 = I_0 \sin \omega_1 t + I_0 \sin \omega_2 t \quad (2.2)$$

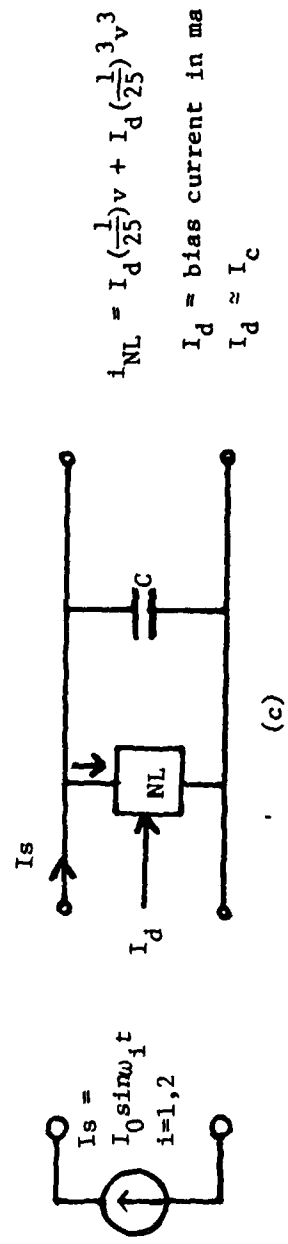
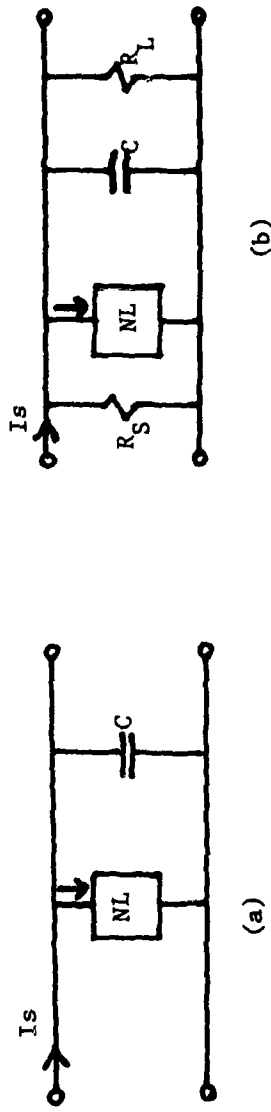


FIGURE 2.1 - NONLINEAR SYSTEMS THAT WERE ANALYZED

Introducing a dimensionless parameter μ before the nonlinear term results in:

$$\frac{dv}{dt} = -Av - \mu Bv^3 + AE_0 \sin \omega_1 t + AE_0 \sin \omega_2 t \quad (2.3)$$

where $A = a/C$ and $B = b/C$, and $E_0 = I_0 a$ volts.

The solution is of the form:

$$v = v_0(t) + \mu v_1(t)$$

Introducing this into (2.3), and retaining only the zero-order and first-order perturbation terms results in:

$$\dot{v}_0 + \mu \dot{v}_1 + \mu^2 \dot{v}_2 = -Av_0 - \mu Av_1 - \mu Bv_0^3 \quad (2.4)$$

The generating solution (zero-order) is found from the terms having μ raised to the zero power,

$$\mu^0: \dot{v}_0 = -Av_0 + AE_0 \sin \omega_1 t + AE_0 \sin \omega_2 t$$

The steady-state solution to this is:

$$v_0 = \frac{E_0 A}{(A^2 + \omega_1^2)^{1/2}} \cos(\omega_1 t + \phi_1) + \frac{E_0 A}{(A^2 + \omega_2^2)^{1/2}} \cos(\omega_2 t + \phi_2)$$

The first-order* correction term is found from the terms of (2.4) having μ raised to the first power,

$$\mu^1: \dot{v}_1 = -Av_1 - Bv_0^3$$

Expanding, using trigonometric identities, and retaining only third-order* intermodulation terms results in:

$$\begin{aligned} \dot{v}_1 + Av_1 = & -\frac{3}{4} B E_0^3 \left[\frac{A^2}{(A^2 + \omega_1^2)} \cdot \frac{A}{(A^2 + \omega_2^2)^{1/2}} \cos\{(2\omega_1 - \omega_2)t + \phi_3\} \right. \\ & \left. + \frac{A}{(A^2 + \omega_1^2)^{1/2}} \cdot \frac{A^2}{(A^2 + \omega_2^2)} \cos\{(2\omega_2 - \omega_1)t + \phi_4\} \right] \end{aligned}$$

The solution of this is:

*First-order refers to the order of the approximation. The third-order intermodulation product refers to a frequency term, not a third-order approximation.

$$v_1 = -\frac{3}{4}BE_0^3 \left[\frac{A^2}{(A^2 + \omega_1^2)} \cdot \frac{A}{(A^2 + \omega_2^2)^{1/2}} \cdot \frac{1}{((A^2 + (2\omega_1 - \omega_2)^2)^{1/2}} \cdot \cos\{(2\omega_1 - \omega_2)t + \phi_5\} \right. \\ \left. + \frac{A}{(A^2 + \omega_1^2)^{1/2}} \cdot \frac{A^2}{(A^2 + \omega_2^2)} \cdot \frac{1}{((A^2 + (2\omega_2 - \omega_1)^2)^{1/2}} \cos\{(2\omega_2 - \omega_1)t + \phi_6\} \right] \quad (2.5)$$

Note that the coefficients of the solution (2.5) can be generated by cascading a series of lowpass filters with a cutoff frequency of A. An operational way to generate this solution is shown in Figure 2.2. Variation of source and load impedance, or of bias current, affects only the cutoff frequency. Results for specific values of load and source impedance, and for various bias current levels, are shown in Table 2.1.

The Volterra series approach is now applied to a second-order (Square law) nonlinearity to show that its solution can also be represented by a combination of filters and multipliers. Consider again the nonlinear circuit shown in Figure 2.1a. Let the behavior across the nonlinear element be described by:

$$i_{NL} = av + bv^2$$

The system differential equation is:

$$i(t) = C \frac{dv}{dt} + G_1 v(t) + G_2 v^2(t)$$

In general, let the input to the system be a sum of exponentials

$$x(t) = \sum_{k=1}^K A_k e^{(j\omega_k t)}$$

According to the Volterra series approach, the n-th order impulse response is given by Equation (2.6).

$$y_n(t) = \sum_{k_1=1}^K \sum_{k_2=1}^K \dots \sum_{k_n=1}^K \left[\left(\prod_{i=1}^n A_{k_i} \right) H_n(j\omega_{k_1}, j\omega_{k_2}, \dots, j\omega_{k_n}) \right. \\ \left. x e^{j(\omega_{k_1} + \omega_{k_2} + \dots + \omega_{k_n})t} \right] \quad (2.6)$$

To determine the first-order nonlinear transfer function, let $i(t) = \exp(j\omega_1 t)$. Using (2.6) with $n=1$, $A_K=1$,

$$v_1(t) = \sum_{K_1=1}^1 H_1(j\omega_{K_1}) e^{j\omega_{K_1} t}$$

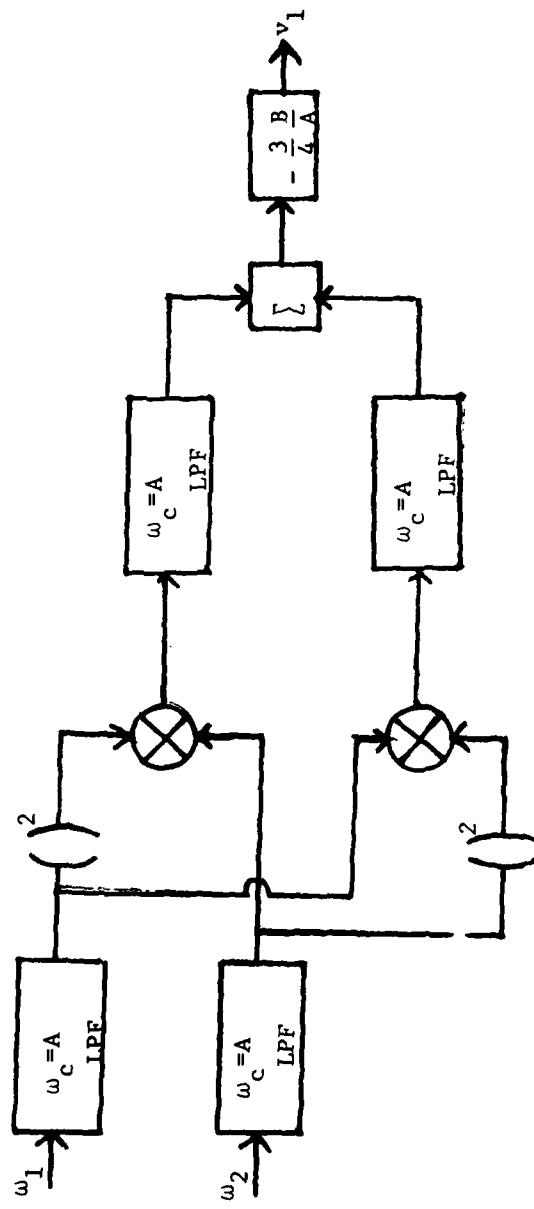


FIGURE 2.2 - OPERATIONAL MODEL

Table 2.1 - Numerical Examples

C	R_S	R_L	Bias Current (mA)	Difference between Upper and Lower Third-Order IMP
159 pF	X	X	X	8 dB
159 pF	50	50	X	6 dB
159 pF	X	X	0.02	15 dB
159 pF	X	X	0.25	15 dB
159 pF	X	X	2.5	8 dB

X = not in circuit

$$\omega_1 = 6.28 \times 10^8 \text{ rads/sec}$$

$$\omega_2 = 9.42 \times 10^8 \text{ rads/sec}$$

$$a = (1/10) \text{ ohms}^{-1}$$

$$b = (1/1000) \text{ volts}^{-1} \text{ ohms}^{-1}$$

or

$$v_1(t) = H_1(j\omega_1) e^{j\omega_1 t}$$

Substituting into the differential equation

$$e^{j\omega_1 t} = Cj\omega_1 H_1(j\omega_1) e^{j\omega_1 t} + G_1 H_1(j\omega_1) e^{j\omega_1 t}$$

or

$$H_1(j\omega_1) = \frac{1}{j\omega_1 C + G_1}$$

The first-order solution is that of a linear lowpass filter.

The second-order solution is found by letting $i(t) = \exp(j\omega_1 t) + \exp(j\omega_2 t)$, $K=2$, $n = 1, 2$, $A_1 = A_2 = 1$, and $v(t) = v_1(t) + v_2(t)$. Using Equation (2.6) with $n=1$

$$v_1(t) = \sum_{K_1=1}^2 H_1(j\omega_{K_1}) e^{j\omega_{K_1} t}$$

or

$$v_1(t) = H_1(j\omega_1) e^{j\omega_1 t} + H_1(j\omega_2) e^{j\omega_2 t}$$

Substituting this into the system differential equation

$$\begin{aligned} e^{j\omega_1 t} + e^{j\omega_2 t} &= C[j\omega_1 H_1(j\omega_1) e^{j\omega_1 t} + j\omega_2 H_1(j\omega_2) e^{j\omega_2 t}] \\ &+ G_1 [H_1(j\omega_1) e^{j\omega_1 t} + H_1(j\omega_2) e^{j\omega_2 t}] \\ &+ G_2 [H_1(j\omega_1) e^{j\omega_1 t} + H_1(j\omega_2) e^{j\omega_2 t}]^2 \end{aligned}$$

Squaring, condensing like terms, and solving for $H_1(j\omega_2)$ results in

$$H_1(j\omega_2) = \frac{1}{j\omega_2 C + G_1}$$

$v_2(t)$ is obtained with $K=2$, $n=2$. Using Equation (2.6),

$$\begin{aligned} v_2(t) &= \sum_{K_1=1}^2 \sum_{K_2=1}^2 H_2(j\omega_{K_1}, j\omega_{K_2}) e^{j(\omega_{K_1} + \omega_{K_2})t} \\ &= \sum_{K_1=1}^2 [H_2(j\omega_{K_1}, j\omega_1) e^{j(\omega_{K_1} + \omega_1)t} + H_2(j\omega_{K_1}, j\omega_2) e^{j(\omega_{K_1} + \omega_2)t}] \end{aligned}$$

or

$$v_2(t) = H_2(j\omega_1, j\omega_1) e^{j2\omega_1 t} + H_2(j\omega_1, j\omega_2) e^{j(\omega_1 + \omega_2)t} \\ + H_2(j\omega_2, j\omega_1) e^{j(\omega_1 + \omega_2)t} + H_2(j\omega_2, j\omega_2) e^{j2\omega_2 t}$$

Substituting v_2 into the differential equation results in:

$$e^{j\omega_1 t} + e^{j\omega_2 t} = C [j2\omega_1 H_2(j\omega_1, j\omega_1) e^{j2\omega_1 t} + j(\omega_1 + \omega_2) H_2(j\omega_1, j\omega_2) e^{j(\omega_1 + \omega_2)t} \\ + j(\omega_1 + \omega_2) H_2(j\omega_2, j\omega_1) e^{j(\omega_1 + \omega_2)t} \\ + j2\omega_2 H_2(j\omega_2, j\omega_2) e^{j2\omega_2 t}] \\ + G_1 [H_2(j\omega_1, j\omega_1) e^{j2\omega_1 t} + H_2(j\omega_1, j\omega_2) e^{j(\omega_1 + \omega_2)t} \\ + H_2(j\omega_2, j\omega_1) e^{j(\omega_1 + \omega_2)t} + H_2(j\omega_2, j\omega_2) e^{j2\omega_2 t}] \\ + G_2 [H_2(j\omega_1, j\omega_1) e^{j2\omega_1 t} + H_2(j\omega_1, j\omega_2) e^{j(\omega_1 + \omega_2)t} \\ + H_2(j\omega_2, j\omega_1) e^{j(\omega_1 + \omega_2)t} + H_2(j\omega_2, j\omega_2) e^{j2\omega_2 t}]^2$$

Squaring, and equating coefficients of $e^{j(\omega_1 + \omega_2)t}$, results in

$$0 = 2G_2 H_1(j\omega_1) H_1(j\omega_2) + 2 [j(\omega_1 + \omega_2) C + G_1] H_2(j\omega_1, j\omega_2)$$

Solving for $H_2(j\omega_1, j\omega_2)$:

$$H_2(j\omega_1, j\omega_2) = -G_2 H_1(j\omega_1) H_1(j\omega_2) H_1 [j(\omega_1 + \omega_2)]$$

Since $H_1(j\omega_1)$ and $H_1(j\omega_2)$ are known,

$$H_2(j\omega_1, j\omega_2) = \frac{-G_2}{(j\omega_1 C + G_1)(j\omega_2 C + G_2) [j(\omega_1 + \omega_2) C + G_1]}$$

$H_2(j\omega_1, j\omega_2)$ is the second-order, nonlinear transfer function of the nonlinear circuit. This solution agrees with the solution obtained using a perturbation technique (but not shown here).

3.0 CHARACTERIZATION STUDIES OF NONLINEARITIES

Characterization of nonlinearities is essential in the development of automatic nonlinear cancellation systems. In most instances, a reference of the nonlinear interference cannot be obtained. Therefore, a nonlinear reference must be synthesized using a nonlinearity similar to that of the interfering nonlinearity. Characterization studies are necessary to identify features of nonlinearities that lead to good nonlinear cancellation.

Many techniques have been used in an attempt to characterize nonlinear devices. Most often, the measurement of device nonlinearity has been determined using two-tone tests. Using this method, two sinusoids are input into a device at separate frequencies and at a prescribed power level. Typically, the second- or third-order IM products are monitored. The amplitudes of the fundamental signals and distortion products are compared, and the second- or third-order intercept points calculated. This technique suffers from two major drawbacks. First, because it is impractical to scan all possible frequency combinations using discrete frequencies, IM distortion at critical frequency combinations may not be observed. Second, all n-th order IMP products cannot be generated using discrete frequency inputs.

An alternate technique utilizes notched bandlimited noise to excite the nonlinear device under test. When third-order distortion is to be measured, the noise bandwidth should be less than f_0 , where f_0 is the center frequency of the notch. If the bandwidth is larger than f_0 , second- and third-order terms will appear in the notch, making it impossible to isolate the third-order behavior of the nonlinear device. Furthermore, notch width must be kept below one-tenth of the bandwidth of the input spectrum to minimize the loss of IM products. Figure 3.1 shows the spectrum from noise of spectral density N and bandwidth B centered about f_0 .

3.1 TWO-TONE MEASUREMENTS OF THE THIRD-ORDER INTERCEPT AS A FUNCTION OF INPUT POWER

Consider a two-tone signal of equal amplitude $v_1 = A(\cos \omega_1 t + \cos \omega_2 t)$ that is input into a nonlinearity of the form.

$$v_0 = K_1 v_1 + K_2 v_1^2 + K_3 v_1^3 \quad (3.1)$$

It can be easily shown that applying v_1 to Equation (3.1) results in third-order intermodulation products

$$v_0 = (3/4)K_3 A^3 [\cos[(2\omega_1 - \omega_2)t] + \cos[(2\omega_2 - \omega_1)t]]$$

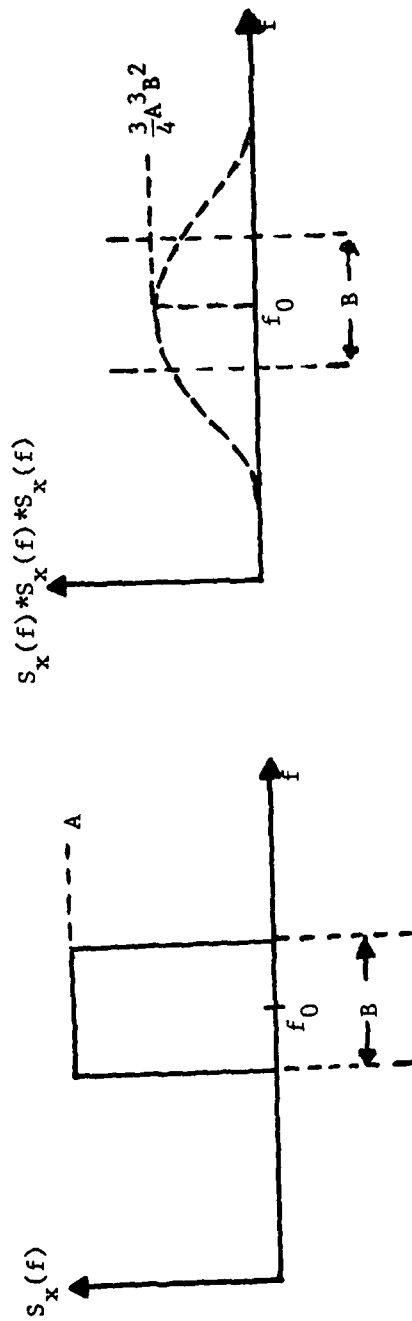


FIGURE 3.1 - TRIPLE CONVOLUTION PRODUCT GENERATED WHEN BANDLIMITED NOISE PASSES THROUGH A THIRD-ORDER NONLINEARITY

The third-order intercept point of a device (I_3) is defined as the output power level at which the power at the frequency $(2\omega_1 - \omega_2)$ or $(2\omega_2 - \omega_1)$ would intercept the output power at ω_1 or ω_2 when low power levels are extrapolated (Figure 3.2). The third-order intercept point can be calculated using

$$I_3 = [(P - P_{IMP})/2] + P$$

where P = power of tone

P_{IMP} = power of third-order intermodulation product at $(2\omega_1 - \omega_2)$ or $(2\omega_2 - \omega_1)$

This equation is valid only when the power of the two-tone input is well below the 1 dB compression point of the device under test. Note that for a third-order device, IMP power is directly proportional to the cube of the input power.

The test setup to measure I_3 for an FH1100 Schottky diode is shown in Figure 3.3. The generators were sufficiently isolated so that the third-order products (IMP_3) were down 80 dB at the output when the nonlinearity was removed.³ Third-order intercept as a function of power per tone is shown in Figure 3.4. Note that as power is increased, the apparent third-order intercept is reduced in level. This occurs because the diode saturates and no longer exhibits strict third-order behavior.

3.2 NOTCHED NOISE MEASUREMENTS OF INTERMODULATION DISTORTION

Notched bandlimited noise was then used to excite the device under test (DUT) as shown in Figure 3.5. Attenuators A-1 and A-2 were used so that the power level at the DUT could be varied while keeping the power level at the spectrum analyzer constant. A1+A2 was set to equal 12 dB. Results are shown in Figure 3.6 for output power from -7 to -1 dBm total power in 1 dB steps. Compression of the intermodulation products at higher power range indicates that the DUT is behaving as a strong nonlinearity.

In many cases, it is desirable to predict the magnitude of the IMPs generated by a noise input into a nonlinear device by using the device's two-tone response. This was accomplished by using correction factor K in the equation below.

$$K = P + [(P_d - IMP_d)/2] - I_3$$

where P_d = noise density in the center of the notch
 IMP_d = intermod product density within the notch
 P = half the noise power
 I_3 = third-order intercept for the DUT excited by a two-tone.

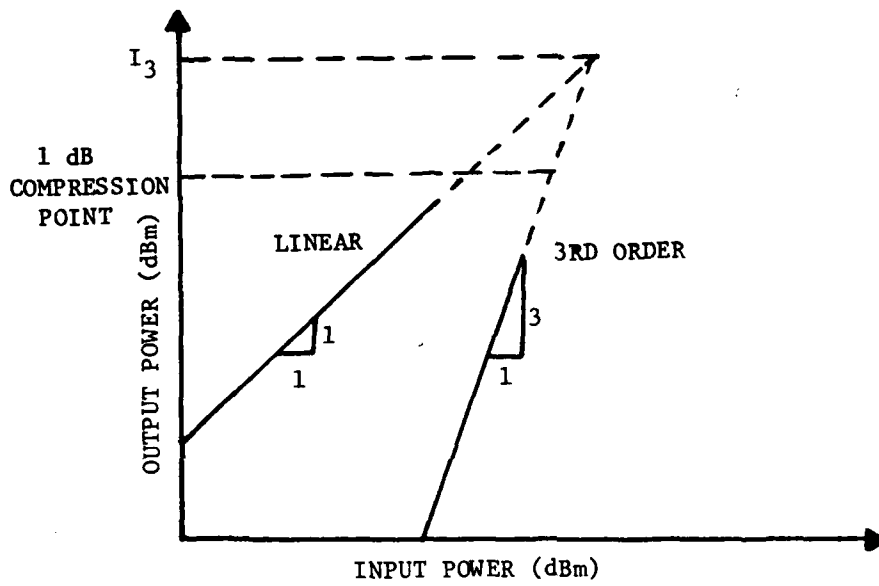


FIGURE 3.2 - DEFINITION OF THIRD-ORDER INTERCEPT POINT (I_3)

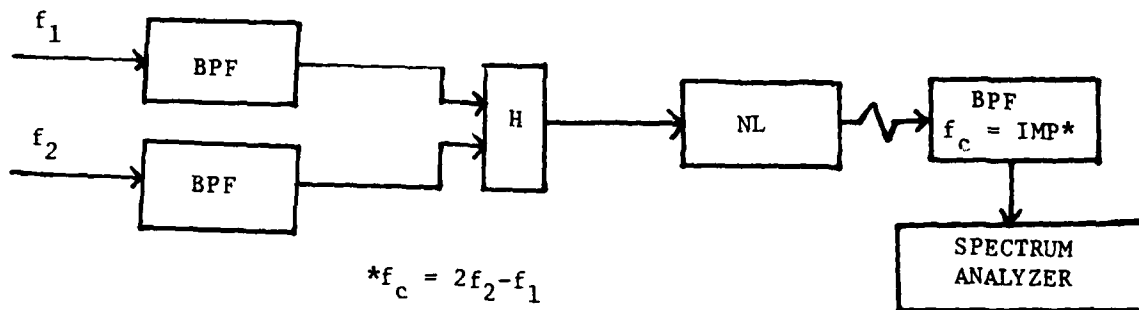


FIGURE 3.3 - SYSTEM TO MEASURE THIRD-ORDER INTERCEPT OF A SHUNT FH1100 SCHOTTKY DIODE

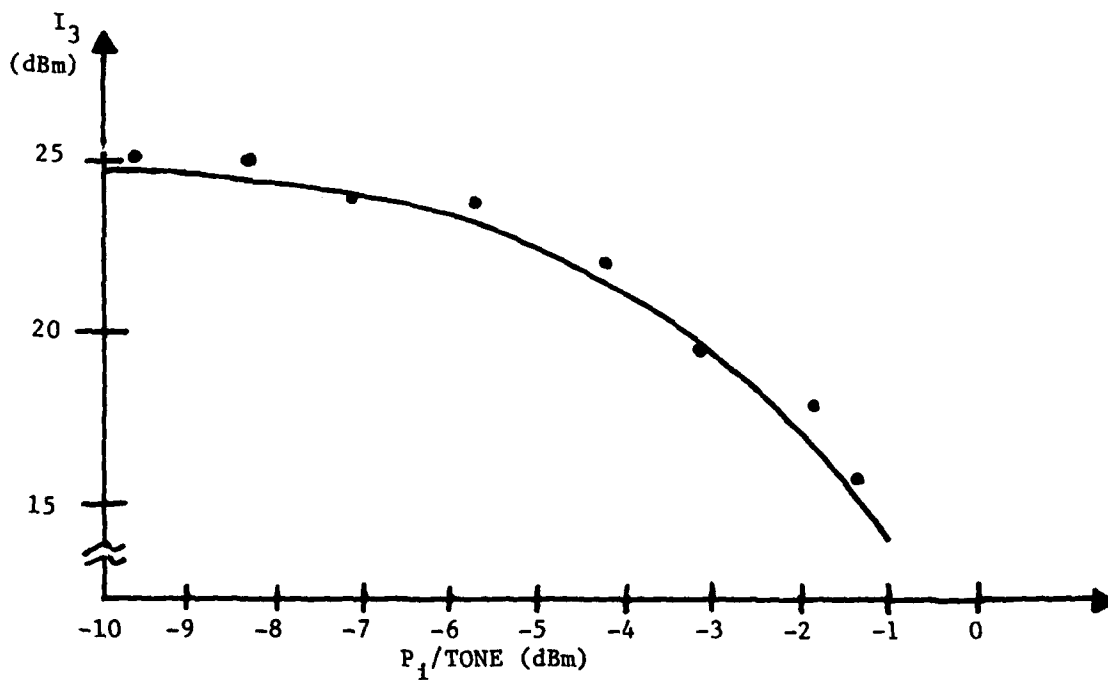


FIGURE 3.4 - THIRD-ORDER INTERCEPT AS A FUNCTION OF POWER PER TONE

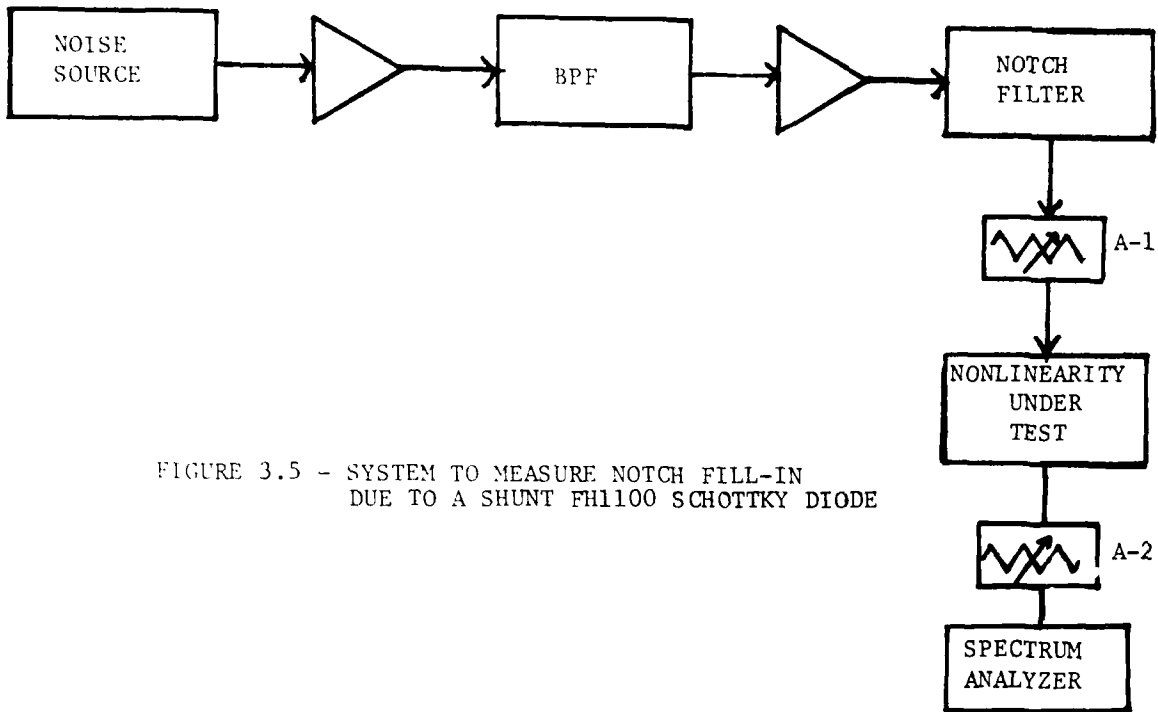
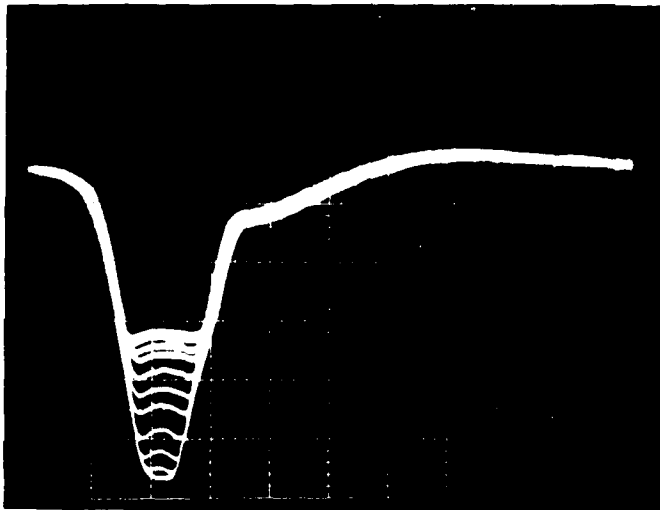


FIGURE 3.5 - SYSTEM TO MEASURE NOTCH FILL-IN
DUE TO A SHUNT FH1100 SCHOTTKY DIODE



10 dB/VERTICAL DIVISION
200 kHz/HORIZONTAL DIVISION
30 kHz RESOLUTION

INPUT POWER CHANGED IN
1 dB STEPS

FIGURE 3.6 - RELATIVE IMP DENSITY AS A FUNCTION OF INPUT POWER
FOR A SINGLE SCHOTTKY DIODE SHUNTED ACROSS A 50-OHM LINE

For an FH-1100 Schottky diode, K was found to be -5 dB. This indicates that an FH-1100 diode generates a greater amount of intermodulation distortion with a noise input than with a two-tone input of equal power. In fact, bandlimited noise generates more intermodulation distortion than does a two-tone signal in any device containing a third-order nonlinearity. This has been shown analytically and experimentally.

3.3 EFFECT OF DIODE BIAS ON INTERMODULATION GENERATION

The impedance characteristics of a biased FH-1100 Schottky diode were measured in order to obtain a better understanding of factors affecting IMP generation. Bias current levels were varied from 0 to 10 mA, and frequency swept from 100 to 400 MHz on a network analyzer. Results are shown on a Smith chart in Figure 3.7. Note that at approximately 3 mA bias, the diode has nearly a 50-ohm impedance. Studies show similar, but not identical, results for a second FH-1100 Schottky diode at the same bias levels.

Figure 3.8 shows the system that was used to study the effect of bias on intermodulation generation for a two-tone input. For a two-tone input, increasing bias current from zero results in an increasing of IMP levels, followed by levelling, and later a decrease to a very small value. Results for various bias currents are shown in Figures 3.9, 3.10, and 3.11. Note that if the proper bias level is selected, either a "hard nonlinearity" (Figure 3.11), a "soft linearity," (Figure 3.9) or asymmetric IMPs (Figure 3.10) can be generated. Asymmetric IMPs suggest the existence of AM-to-PM conversion.

Similar results were obtained when notched bandlimited noise was input into a diode and the bias varied. Results are shown in Figure 3.12. As bias is increased, the amount of notch fill-in increases, levels off, and then decreases. Note that both the operating point on the diode's V-I curve and the characteristic impedance are changed by bias current, and together may explain this phenomenon.

IMPEDANCE COORDINATES—50-OHM CHARACTERISTIC IMPEDANCE

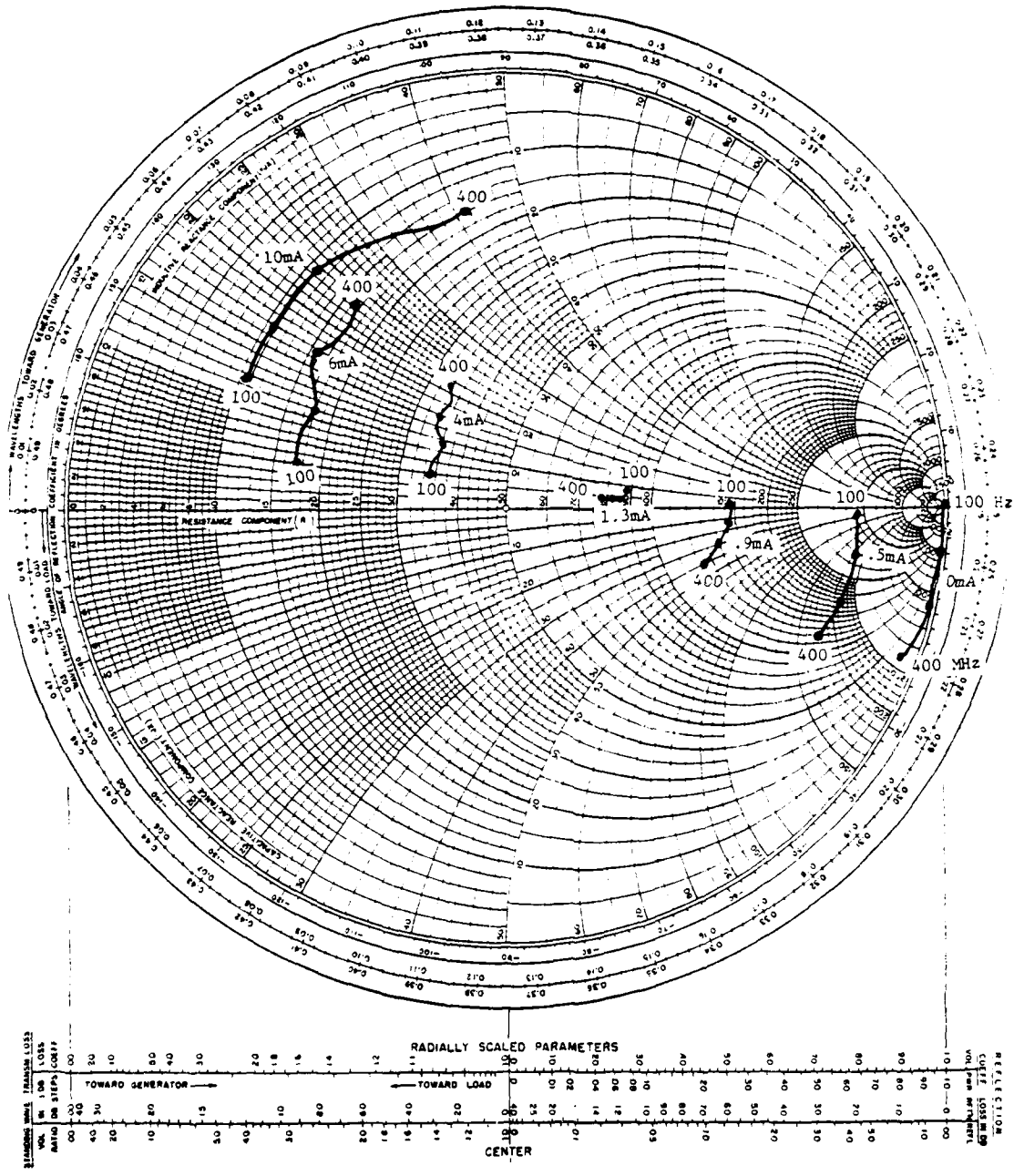


FIGURE 3.7 - IMPEDANCE CHARACTERISTICS OF BIASED FH-1100 SCHOTTKY DIODE AS A FUNCTION OF BIAS CURRENT

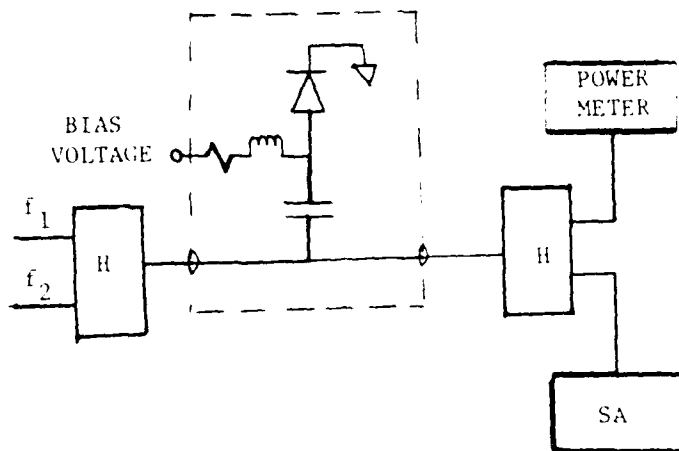


FIGURE 3.8 - SYSTEM USED TO STUDY EFFECT OF BIAS WITH TWO-TONE INPUT

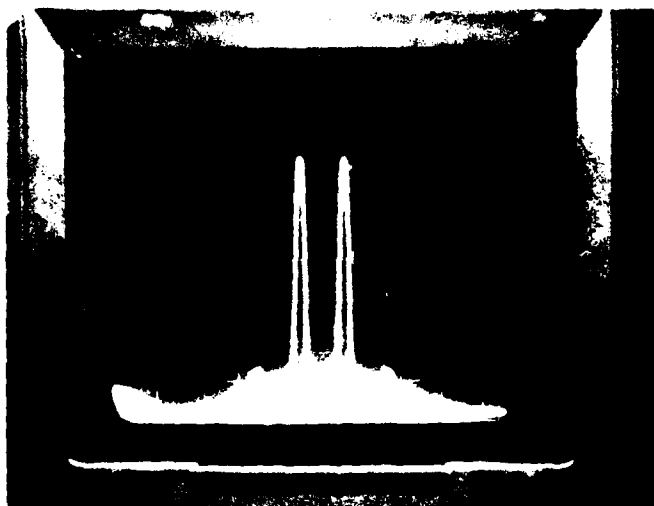


FIGURE 3.9 - LOW BIAS CURRENT

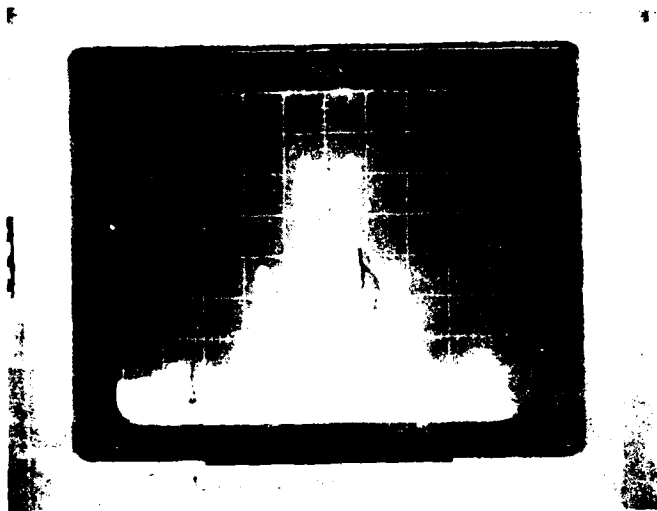


FIGURE 3.10 - ASYMMETRIC FIFTH ORDER IMPS

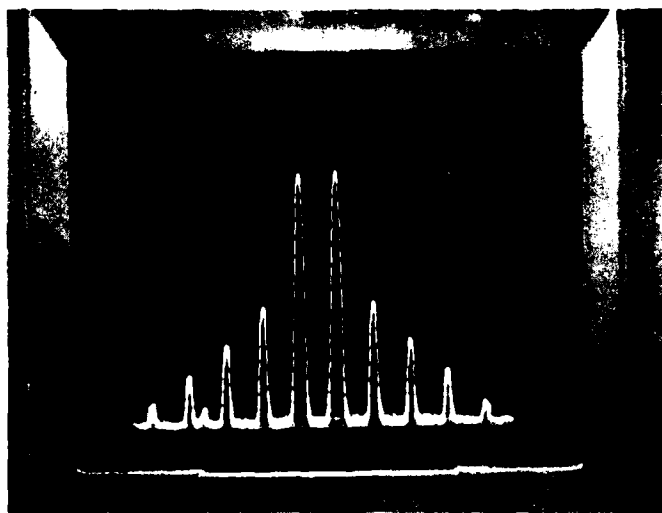
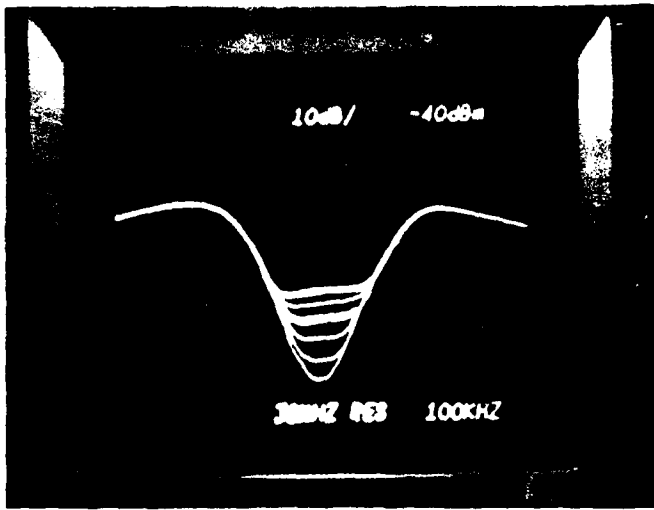
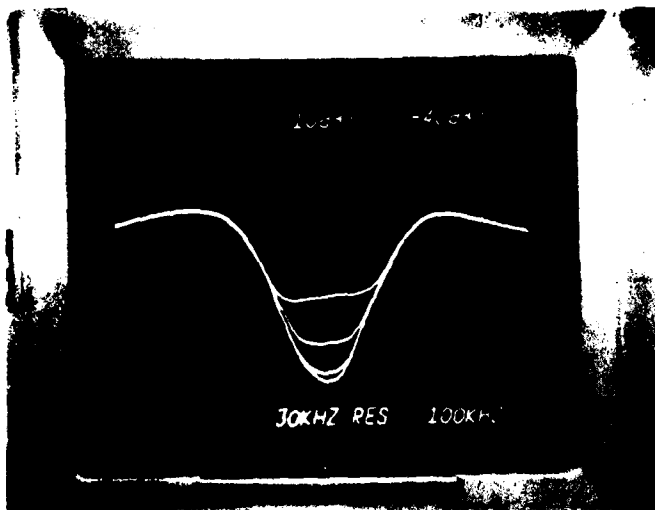


FIGURE 3.11 - BIAS CURRENT ADJUSTED FOR MAXIMUM IMP FORMATION



IMP LEVELS WITH
CURRENT FROM
0 mA TO 3 mA

TOP TRACE = 3 mA
BOTTOM TRACE = 0 mA



IMP LEVELS WITH
CURRENT FROM
3 mA TO 10 mA

TOP TRACE = 3 mA
BOTTOM TRACE = 10 mA

FIGURE 3.12 - IMP VARIATION AS A FUNCTION OF BIAS CURRENT

4.0 NONLINEAR CANCELLATION SYSTEMS

The fundamental operating principle for automatic nonlinear interference cancellers is the same as that of linear cancellers. In both linear and nonlinear cancellers, a portion of the power out of each offending transmitter is diverted to the reference input of the canceller where it is processed to mimic the interfering path that exists between the transmitter(s) and the receiver. Each processed reference is then adjusted in amplitude and phase by a complex weight and combined with the interfering signal incident at the receiver antenna so that cancellation of the interfering signal results. Because the desired signal is not present in the reference, it passes through the cancelling coupler into the receiver unaffected. The error coupler diverts part of the canceller output to the analog weight control loops. This closes the automatic feedback loop.

The major difference between nonlinear cancellers and previous linear cancellers lies in the processing of the reference signal from each transmitter. For good nonlinear cancellation to be obtained, the reference signal must pass through a nonlinear process that mimics the interfering nonlinear process. Important features of this process are the number of nonlinearities, the delay between the reference source and the reference nonlinearities, and the nonlinear characteristics themselves. Since the nonlinear process may be time-varying the nonlinear processor must be adaptive with the ability to change the important features of the process. Control of such a process is best handled by a microprocessor with a suitable control algorithm.

In addition to mimicking the interfering nonlinear process, the nonlinear processor must eliminate the linear signal component so that the nonlinear reference is larger than the linear reference. This is necessary because the LMS algorithm will cancel the largest signal component. Elimination of the linear signal component can be accomplished by using standard linear cancellation techniques, bandpass filters, or a notch filter. Each technique has advantages and disadvantages that will be discussed in later sections.

4.1 MANUAL CANCELLATION

Manual nonlinear cancellation was used during initial studies in order to reduce the complexity of the experimental setup. Generally, a nonlinear reference is generated and manually weighted before it is combined with the nonlinear interference in the canceller coupler. Weight values are adjusted until a minimum interfering output is seen at the spectrum analyzer. A typical system is shown in Figure 4.1.

The primary advantage of manual cancellation in nonlinear cancellation studies is the elimination of feedback control circuitry used to control weight values. The necessity of a good nonlinear reference is also reduced. The disadvantages of manual cancellation in a usable system

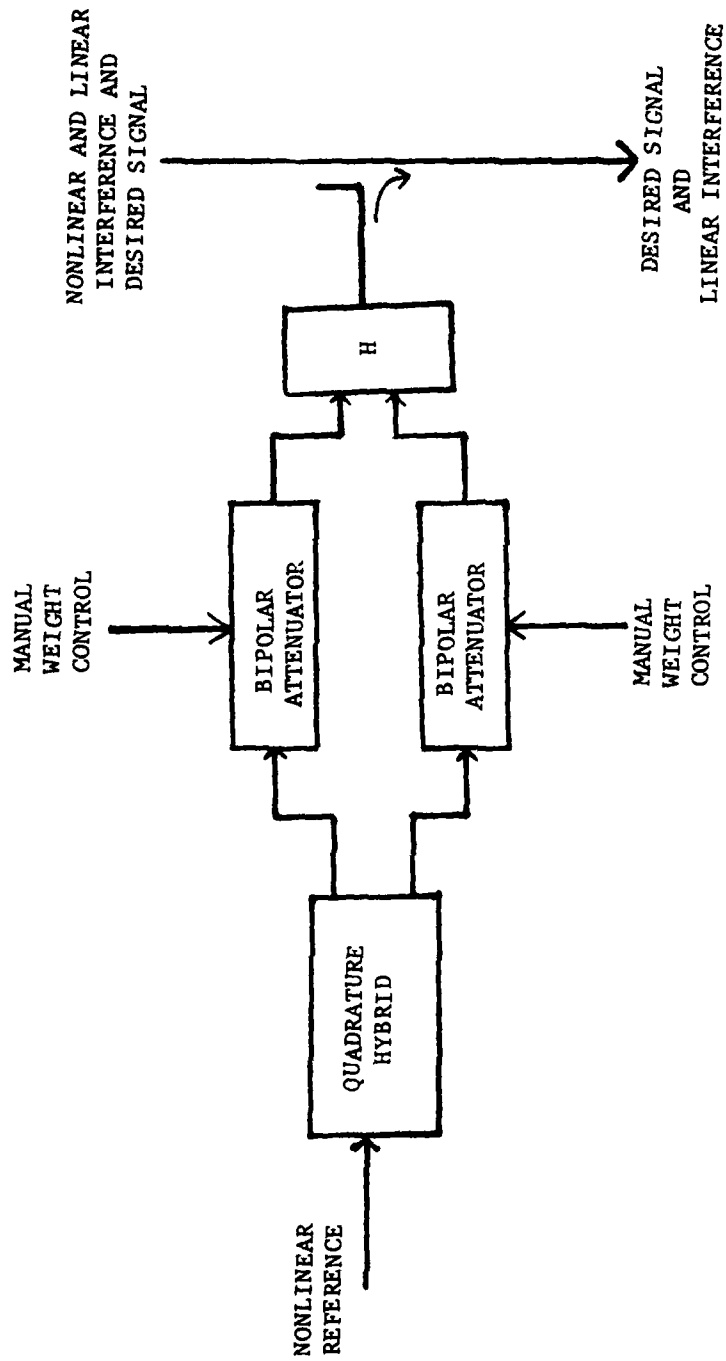


FIGURE 4.1 - MANUAL NONLINEAR CANCELLATION SYSTEM

are its inability to track time-varying changes in the interference, and the difficulty of the manual adjustment process for the user.

4.2 EXPERIMENTAL RESULTS FOR MANUAL NONLINEAR INTERFERENCE CANCELLATION

A number of studies were made using manual nonlinear cancellation techniques. The first study involved the use of the signal reflected from the nonlinearity in an attempt to obtain a nonlinear reference. Other studies investigated the effect of multiple nonlinearities, modulation, or memory on nonlinear cancellation.

One major problem in obtaining good nonlinear cancellation is obtaining a nonlinear reference that matches the interfering nonlinear signal. One possible technique is to obtain a reference from the signal reradiated by the nonlinearity. Such a scheme may be useful when the nonlinearity is near the transmitting antenna (Figure 4.2). A system to simulate this is shown in Figure 4.3. The reflected signal is used as a reference, and the through-path as the interference. The linear signal component is removed by using a notch filter. Results show that greater than 20 dB of nonlinear cancellation can be obtained using this technique (Figure 4.4).

A test was made to establish the mechanism of the degradation involving two nonlinearities. Initially, the two CW tone frequencies were set to 240 MHz and 250 MHz. The manual canceller was set to cancel the intermodulation product at $(2f_2 - f_1) = 260$ MHz (Figure 4.5). The input frequencies were then changed to 250 MHz and 255 MHz, resulting in the same 260 MHz IMP. The cancellation with the new pair of input frequencies degraded to about 5 dB, indicating a sensitivity to dispersion effects ahead of the diodes.

The presence of more than one nonlinearity in the interfering path increases the difficulty of matching the nonlinearity in the reference path. In exploring the feasibility of using an auxiliary antenna for a reference signal, two nonlinearities were excited and each resulting nonlinear signal was sent through two paths to simulate receive and reference antennas. The reference port was coupled into a manual complex weight, as shown in Figure 4.6, and subtracted from the interfering signal. The results in Figure 4.7 show that 16 dB of cancellation can be realized on an intermodulation product when one of the two carriers was 80% amplitude modulated. This test shows only cancellation of two paths originating from the same pair of nonlinearities rather than cancellation between two sets of different nonlinearities.

Multiple nonlinear sources on an aircraft are likely to be at several widely spaced locations. Differences in the delays at which the two interferences arrive at the nonlinearities can lead to differential phase vs frequency slopes. For strictly second- and third-order nonlinearities, however, the resulting intermodulation products are still

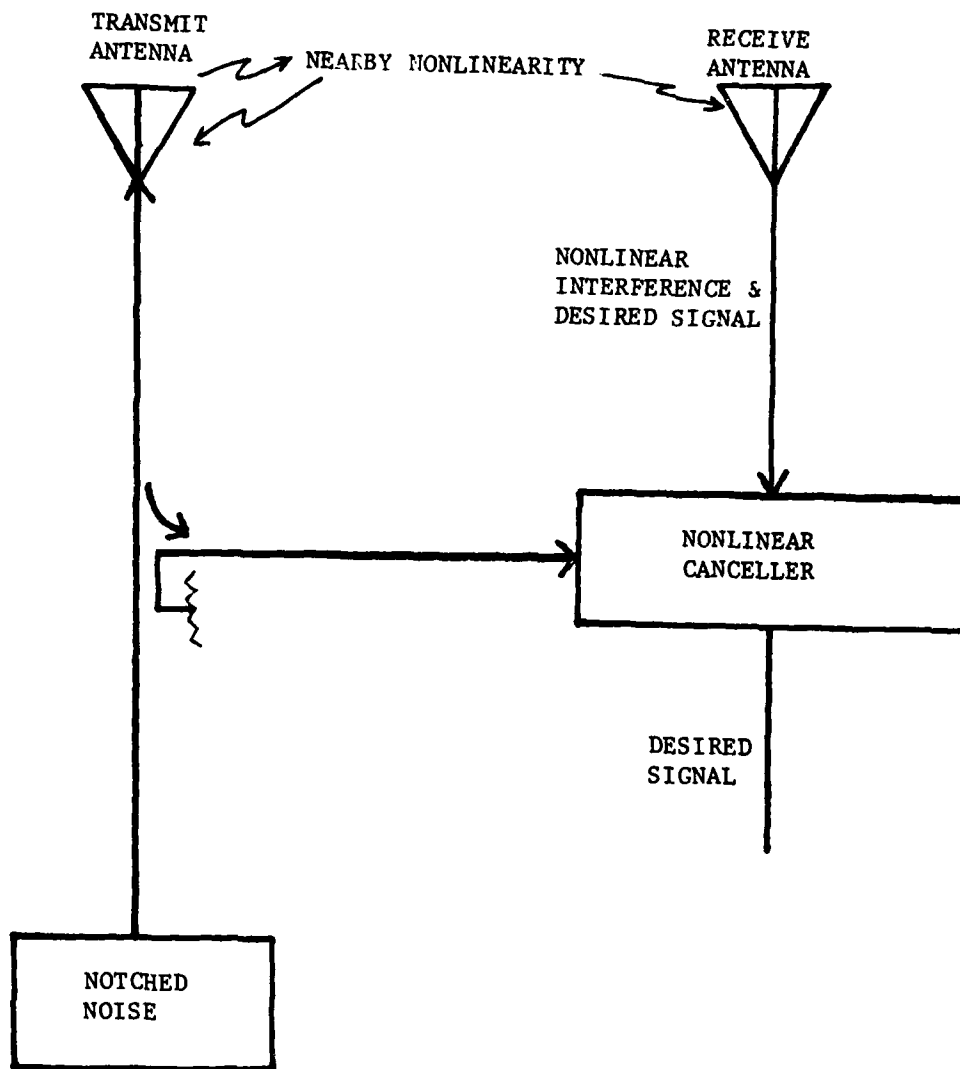


FIGURE 4.2 - NONLINEAR CANCELLATION USING RERADIATED SIGNAL FROM NEARBY NONLINEARITY

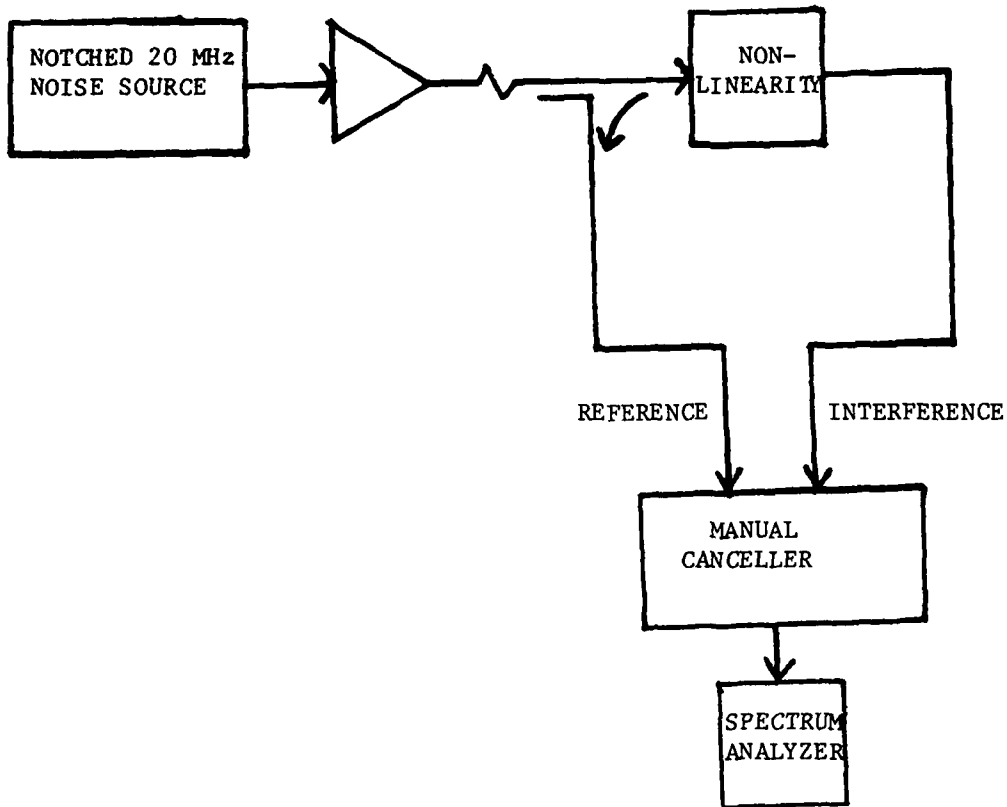
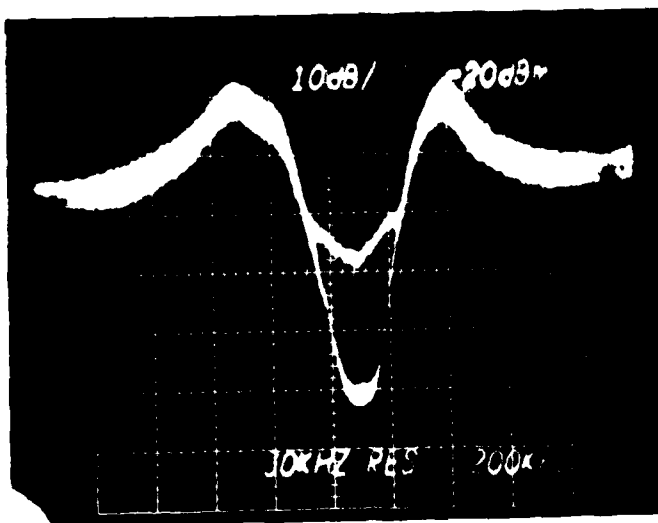


FIGURE 4.3 - SYSTEM USING REFLECTED SIGNAL FOR NONLINEAR REFERENCE



TOP CENTER OF NOTCH =
UNCANCELLED
BOTTOM CENTER OF NOTCH =
CANCELLED

RESULT: 22 dB OF
NONLINEAR CANCELLATION

FIGURE 4.4 - CANCELLATION ACHIEVED USING REFLECTED SIGNAL AS A REFERENCE

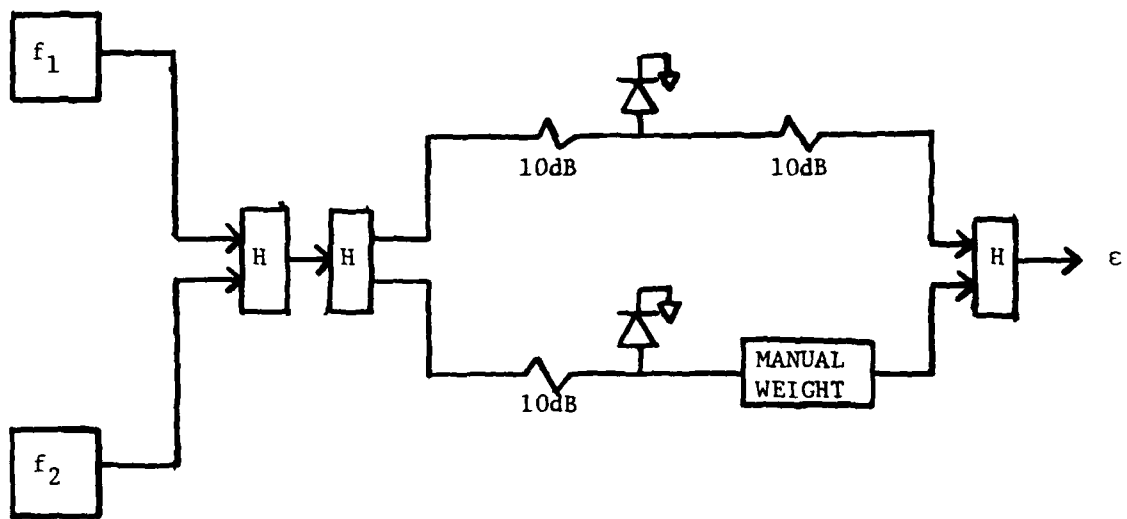


FIGURE 4.5 - SYSTEM TO STUDY DISPERSION EFFECTS

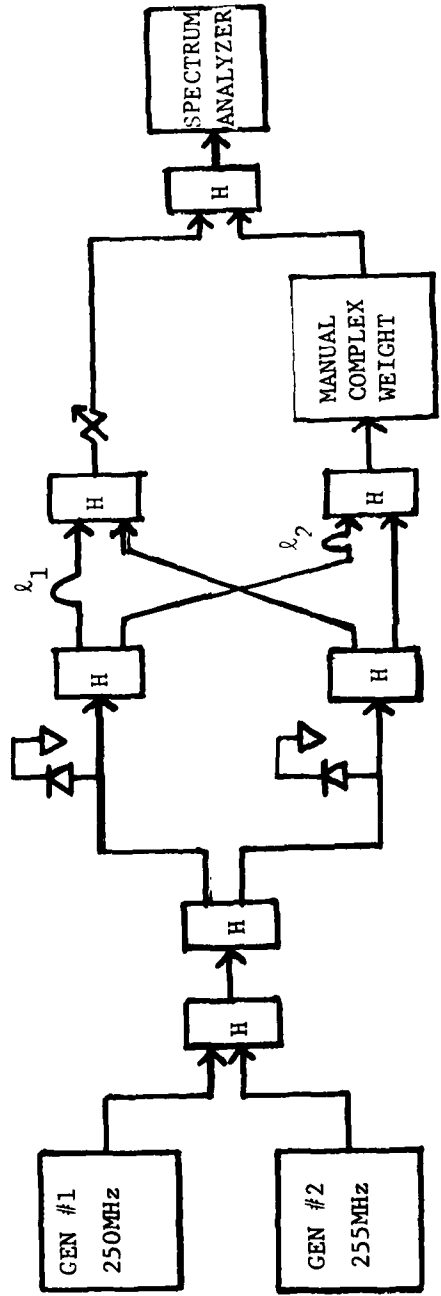
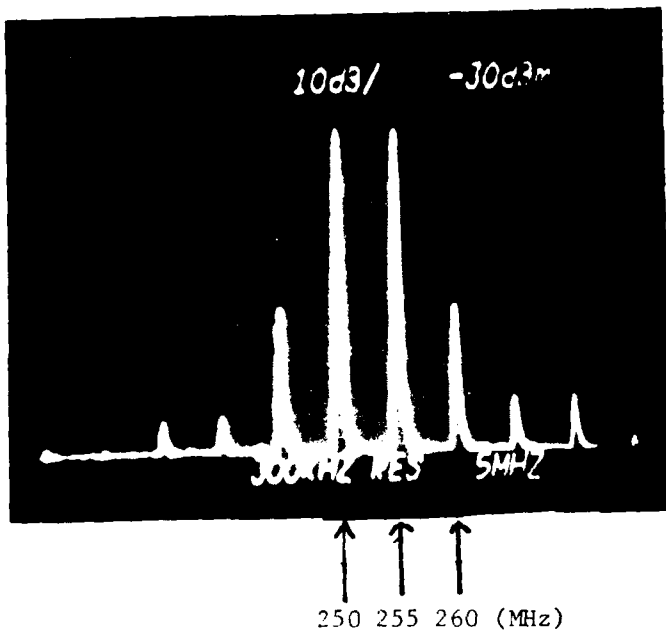
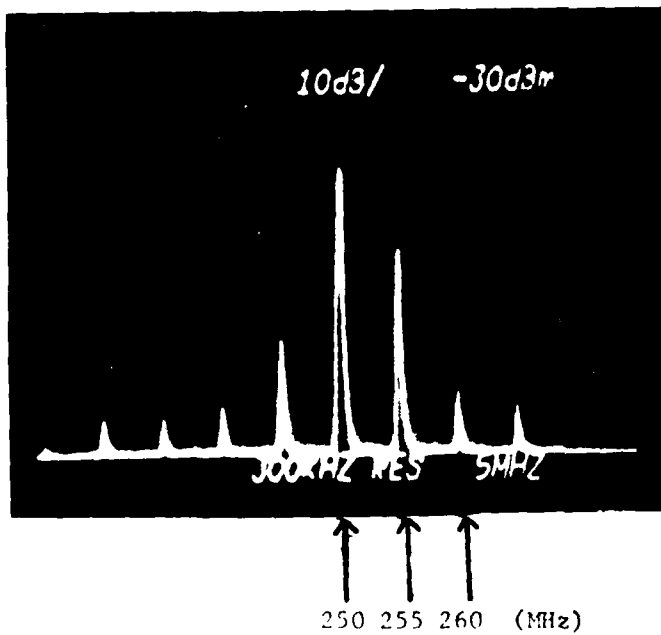


FIGURE 4.6
CONFIGURATION FOR CANCELLATION OF MULTIPLE INTERFERENCES



UNCANCELLED

THIRD-ORDER IMP AT
245 AND 260 MHz



INTERFERENCE PLUS
REFERENCE SHOWING
16 dB CANCELLATION
OF IMP AT 260 MHz.
250 MHz TONE HAS 80%
AM AT 1 kHz

FIGURE 4.7 - CANCELLATION OF A THIRD-ORDER INTERMODULATION PRODUCT ARISING FROM TWO NONLINEARITIES

extremely narrowband compared to the reciprocal of the delay differences. Therefore, only minor effects in cancellation should be expected. Of more importance is the effect of delays on the higher-order products that fall into the second- and third-order product frequency bands and the differences in the amplitude characteristics of the nonlinearities. A test configuration similar to that in Figure 4.6 can be used to determine the severity of variably spaced nonlinearities on cancellation by adjusting line lengths ℓ_1 and ℓ_2 . Results indicate that cable length ℓ_1 and ℓ_2 can be varied 20 feet without degradation in nonlinear cancellation.

The hardness of a nonlinearity depends on the power level of the signal being applied to it (Figure 3.6). It was found that the best nonlinear cancellation was achieved when the power levels incident on the reference and interfering nonlinearity were identical. In terms of nonlinear hardness, this says that every attempt should be made to match the hardness of the reference and interfering nonlinearities. Figure 4.8 contains photographs of manual cancellation of the nonlinear interference generated by a wideband noise process. A deep notch was placed in the noise prior to introduction of the nonlinearity so that the nonlinear contribution would be visible. Notice that the best cancellation occurs when the hardness of the nonlinearities is matched.

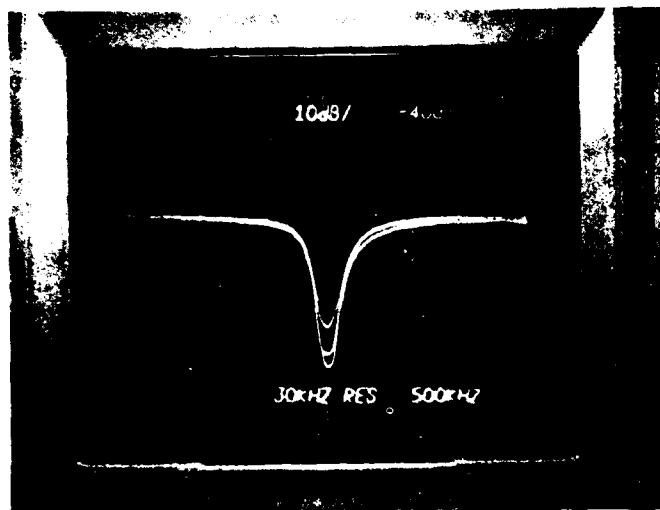
The presence of two or more nonlinearities separated by a time delay creates a memory effect that has been discussed in the previous paragraph. This is really a feed-forward memory effect because it consists of the sum of delayed nonlinear distortions of input waveforms. Of equal importance is a memory effect caused by capacitive properties in nonlinear sources. The most easily discernible feature of a nonlinearity with memory is its ability to create AM-to-PM conversion. In spectral terms, it means that it can change a modulation spectrum that is symmetric (or antisymmetric) about a carrier into one that is asymmetric (neither symmetric nor antisymmetric). This property was shown to exist in biased diodes through a series of experiments performed to characterize the nonlinear properties of Schottky diodes. Figures 3.9 through 3.11 show photographs of intermodulation products generated by a Schottky diode shunted across a transmission line. In the top photograph, no bias is applied to the diode and the intermodulation products are symmetric about the two fundamental tones. In the bottom photograph, a few milliamps of dc current are applied to the diode and the asymmetric intermodulation spectrum results. This occurs because the bias circuit adds a series capacitance to the diode, thereby introducing memory effects. While this creates problems, it can also be exploited to gain more control over the characteristics of a reference nonlinearity. Additional manual nonlinear cancellation has been obtained by adjusting bias on a "soft" reference NL while a "hard" reference NL was used.

Modulation effects on nonlinear cancellation can be studied by applying different forms of narrowband modulation to the two simulated transmitter carriers and applying them to laboratory test configurations.



- UNCANCELLED HARD NONLINEARITY
- HARD INTERFERING NONLINEARITY
CANCELLED BY A HARD REFERENCE
NONLINEARITY
- NO NONLINEARITY

FREQUENCY SPAN = 5 MHz
 CENTER FREQUENCY = 246 MHz



- UNCANCELLED HARD NONLINEARITY
- HARD INTERFERING NONLINEARITY
CANCELLED BY A SOFT REFERENCE
NONLINEARITY
- NO NONLINEARITY

FREQUENCY SPAN = 5 MHz
 CENTER FREQUENCY = 246 MHz

FIGURE 4.8

CANCELLATION OF INTERMODULATION PRODUCTS GENERATED BY
 NONLINEARITIES HAVING VARYING DEGREES OF HARDNESS

Results of an experiment revealed a critical limitation on IMP cancellation due to amplitude modulation, but virtually no limitation due to phase modulation. The test configuration shown in Figure 4.9 was assembled to see how effectively the second-order products of a mixer could be used to cancel the second-order products of a diode shunted across a transmission line.

Figure 4.10 shows that a second-order IMP generated from a CW and FM signal can be cancelled roughly 40 dB across the entire modulation bandwidth by a mixer generated reference IMP. In Figure 4.11, however, the modulation on one carrier is changed to AM while the other carrier remains unmodulated. Notice that the carrier alone is cancelled 20 dB while the sidebands are hardly cancelled at all. The presence of AM on one carrier degrades FM cancellation to roughly 9 dB across the band. Further investigation is needed to examine these effects. IMP is roughly 9 dB across the band.

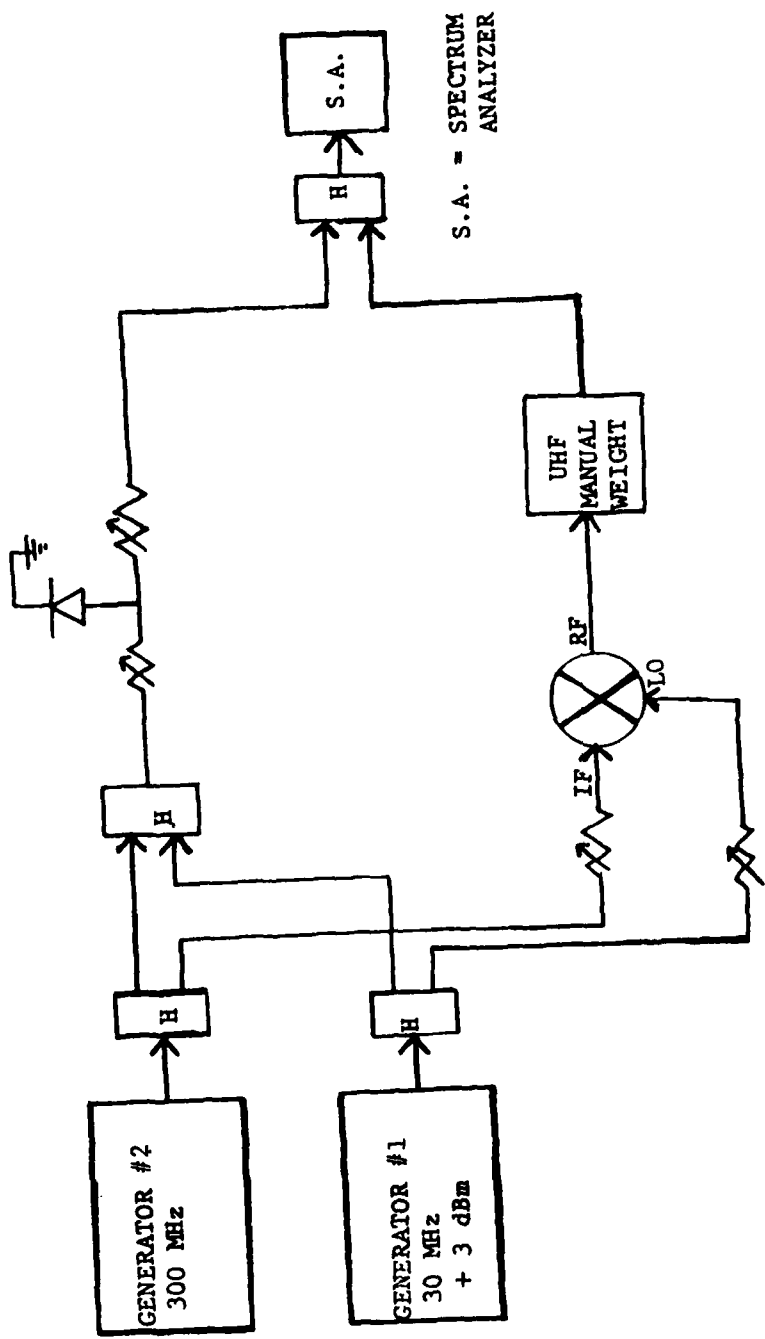
4.3 AUTOMATIC NONLINEAR CANCELLATION

In order to obtain automatic nonlinear cancellation, the nonlinear reference at the correlator must be equal to or larger than the linear signal component. One method to accomplish this is shown in Figure 4.13. This technique involves the use of a notch filter followed by the nonlinearity and a narrow bandpass filter. The frequency spectrum at each point in the system is shown in Figure 4.14.

An automatic nonlinear canceller was implemented that utilized a notch filter followed by narrow bandpass filters to eliminate the linear signal component (Figure 4.15). Notched bandlimited noise is split in a hybrid and impinges on the interfering and reference diode nonlinearities. Notch fill-in then occurs, dependent on the level of IMP generator. The filled notch is then downconverted and passes through a crystal filter with a 100 kHz, 3 dB bandwidth. At the output of the crystal filter, the signal component should be mainly nonlinear. This nonlinear component is then input into a correlator. The output of the correlator is used to automatically set the weights to reduce the nonlinear interference.

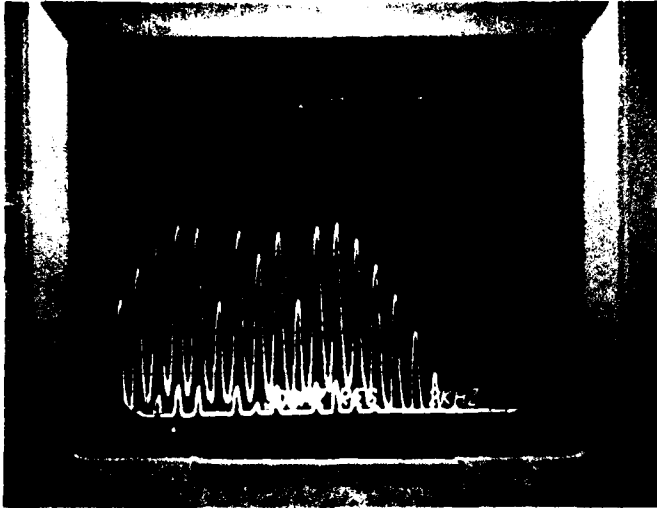
It was found that 10 dB of nonlinear cancellation could be obtained using separate interfering and reference nonlinearities excited by 200 MHz broadband noise (Figure 4.16). Over 32 dB of cancellation was achieved when a single nonlinearity excited by broadband noise was split into interfering and reference paths (Figure 4.17). These results indicate that nonlinear cancellation was limited by the inability to match nonlinear transfer functions, and not by ICS limitations.

Another nonlinear canceller scheme used in a design to protect AFSATCOM receivers is shown in Figure 4.18. This system uses a nonlinear reference generator to reduce the linear signal component below the level of the nonlinear signal component. This is accomplished by using a linear reference and a linear and nonlinear interference in an interference canceller. Figure 4.19 shows the output of the nonlinear reference



S.A. = SPECTRUM ANALYZER

FIGURE 4.9
TEST CONFIGURATION FOR MODULATION EFFECTS ON IMP CANCELLATION



10 dB/DIV

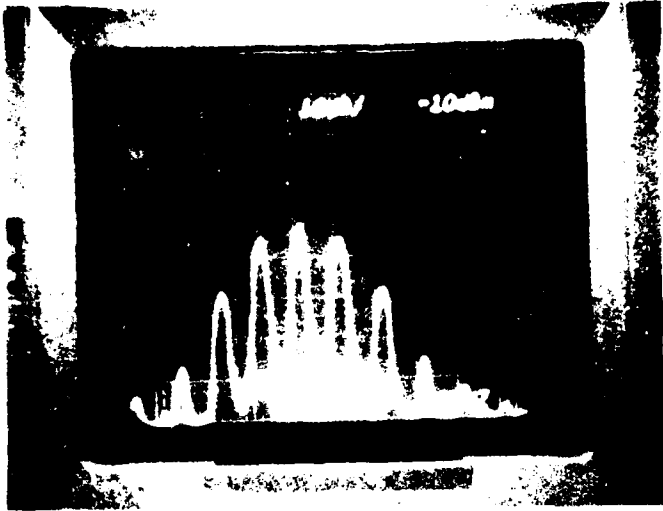
TOP TRACE = UNCANCELLED
IMP

BOTTOM TRACE = CANCELLED
IMP

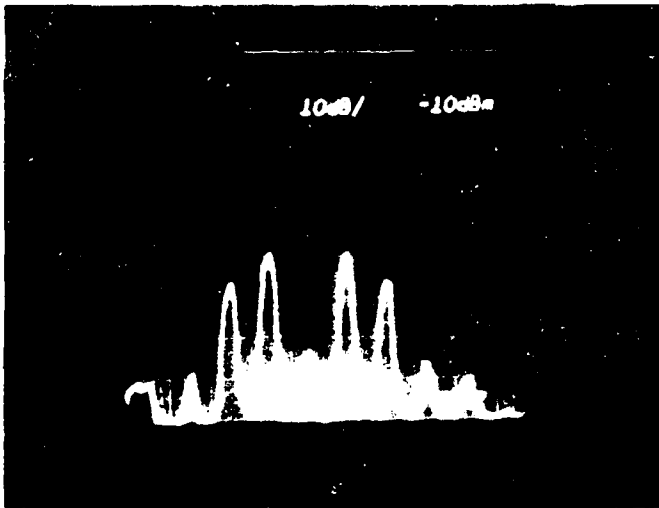
FREQUENCY IN kHz
2 kHz/DIV

FIGURE 4.10

MANUAL CANCELLATION OF A SECOND ORDER HF-CWxUHF-FM IMP.
SIGNAL #2 = 300 MHz FM TONE, 20 kHz DEV AT 1 kHz



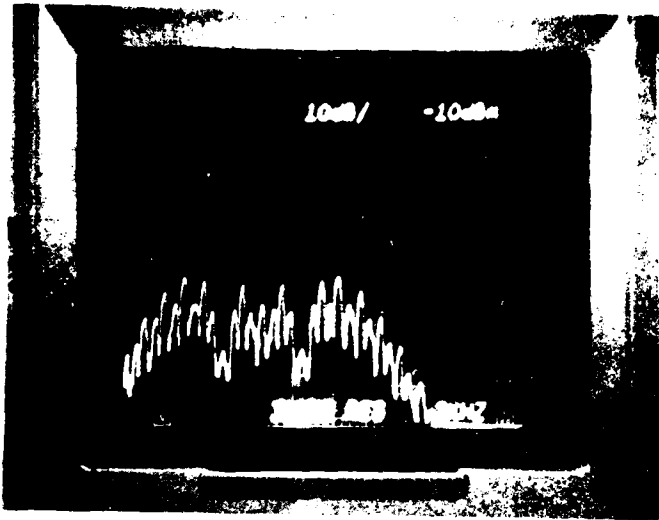
UNCANCELLED IMP



CANCELLED IMP

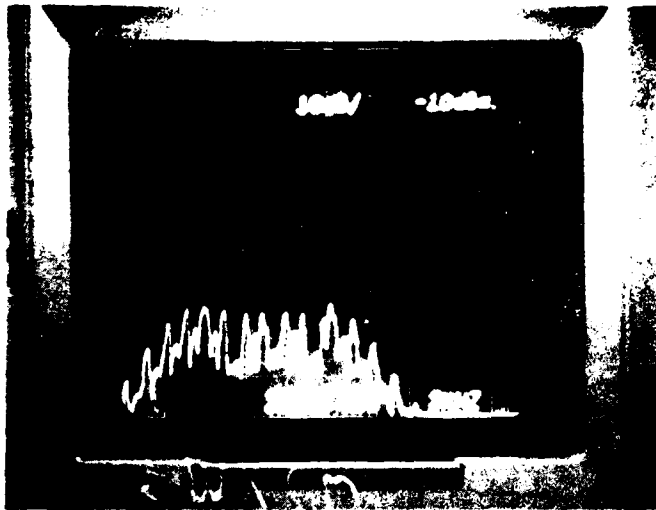
NOTE THAT CARRIER IS
CANCELLED MORE THAN
SIDE BANDS

FIGURE 1. CARRIER CANCELLATION OF A SECOND-ORDER HF-CW
SIGNAL
SIGNAL: 100 MHz 80% AM @ 1 kHz



UNCANCELLED IMP

FREQUENCY IN kHz
2 kHz/DIV



CANCELLED IMP

FREQUENCY IN kHz
2 kHz/DIV

FIGURE 4.12

MANUAL CANCELLATION OF A SECOND ORDER HF-AMxUHF-FM IMP.
SIGNAL #1 = 30 MHz 80% AM @ 1 kHz, SIGNAL #2 = 300 MHz
FM TONE, 20 kHz DEV @ 1 kHz.

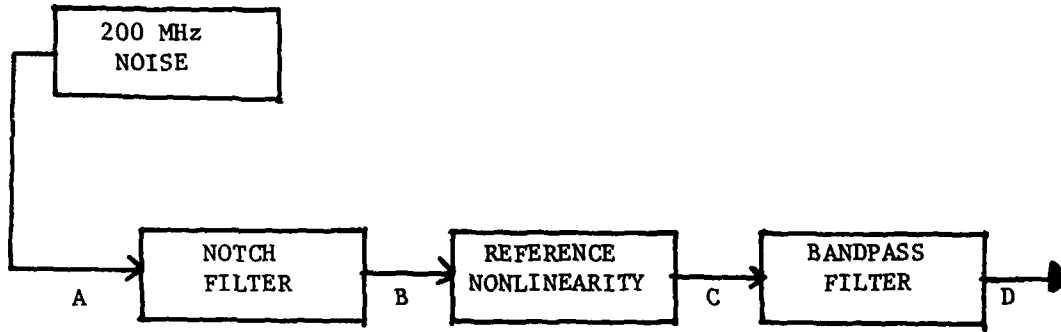


FIGURE 4.13 - USE OF NOTCH FOLLOWED BY BANDPASS FILTER TO OBTAIN NONLINEAR REFERENCE

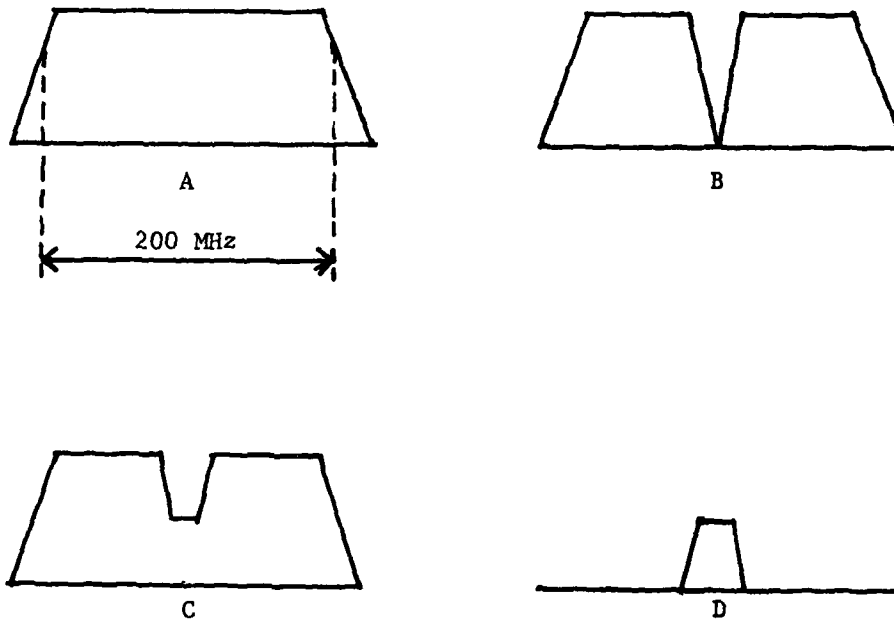
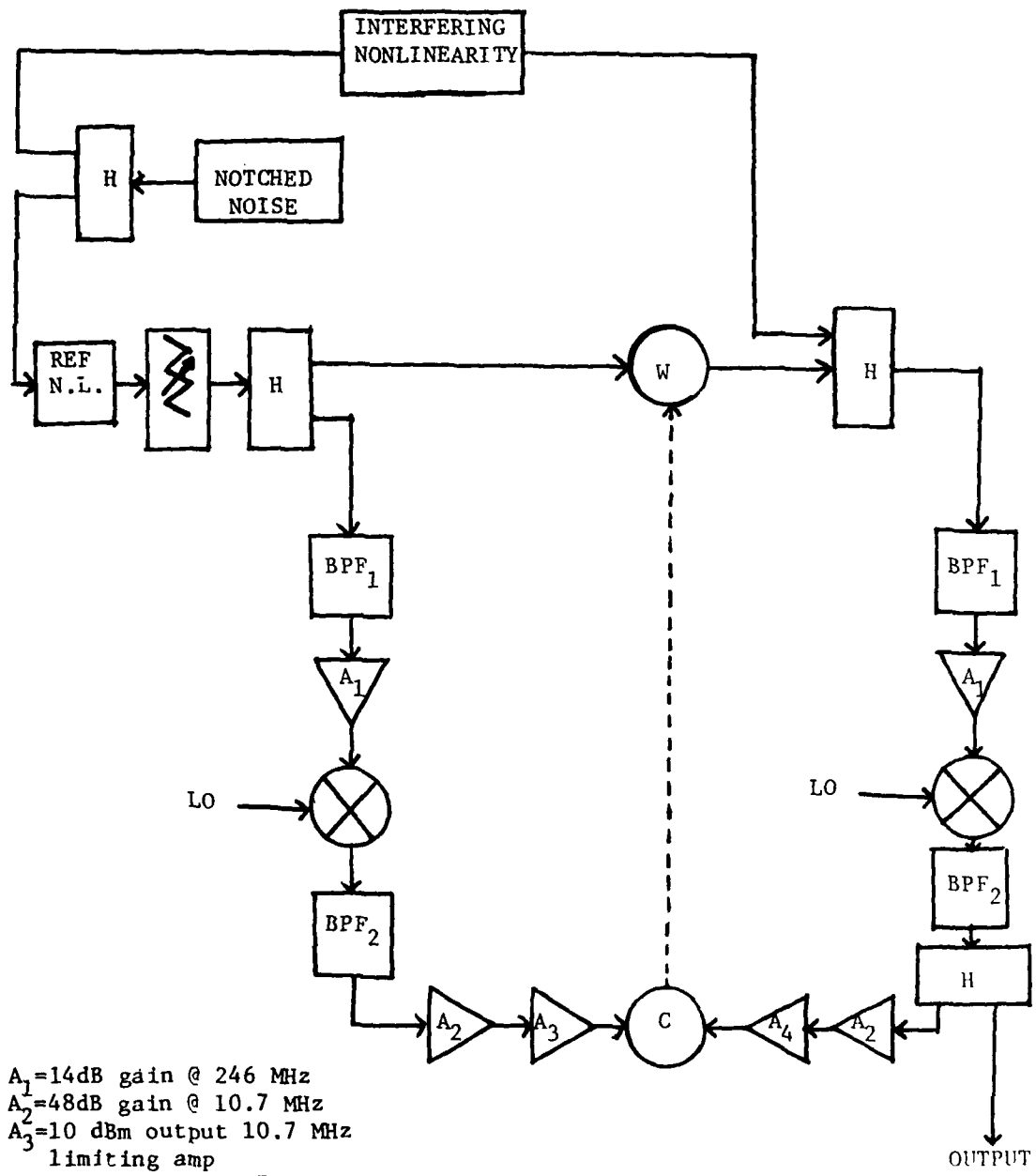
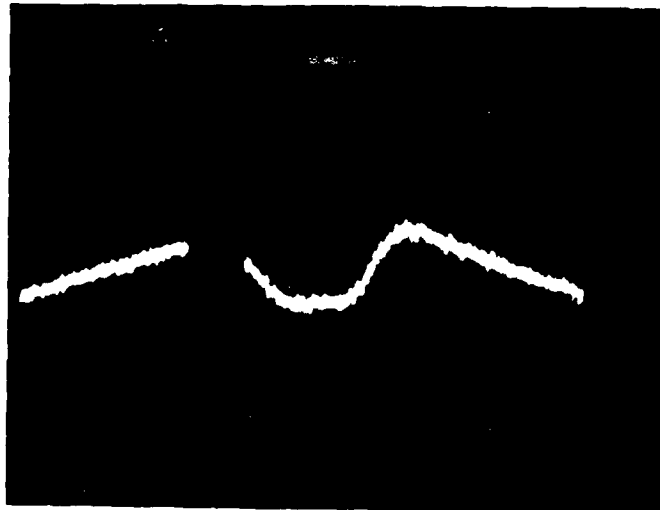


FIGURE 4.14 - FREQUENCY SPECTRUM AT EACH PORTION OF FIGURE 4.12



A_1 = 14dB gain @ 246 MHz
 A_2 = 48dB gain @ 10.7 MHz
 A_3 = 10 dBm output 10.7 MHz limiting amp
 A_4 = 57dB gain @ 10.7 MHz
 BPF_1 : f_c = 246 MHz; 3 dB BW = 300 kHz; 2-pole
 BPF_2 : f_c = 10.7 MHz; 3 dB BW = 100 kHz; 4-pole

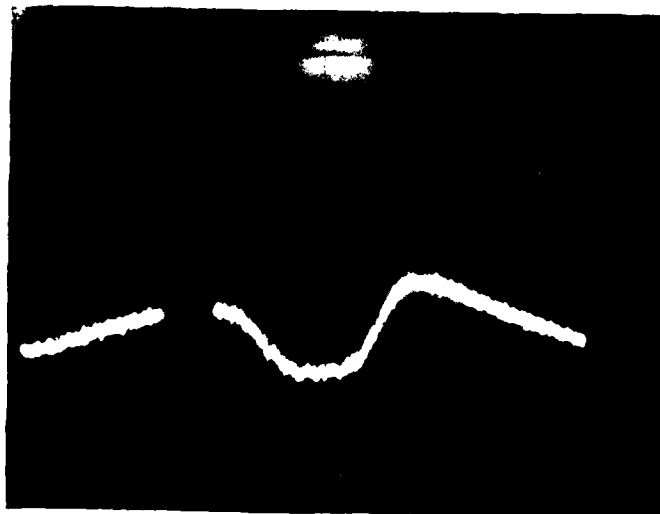
FIGURE 4.15 - AUTOMATIC NONLINEAR CANCELLATION SYSTEM



UNCANCELLED

VERTICAL
SCALE =
10 dB/DIV

CENTER FREQUENCY = 246 MHz
FREQUENCY SPAN = 2 MHz

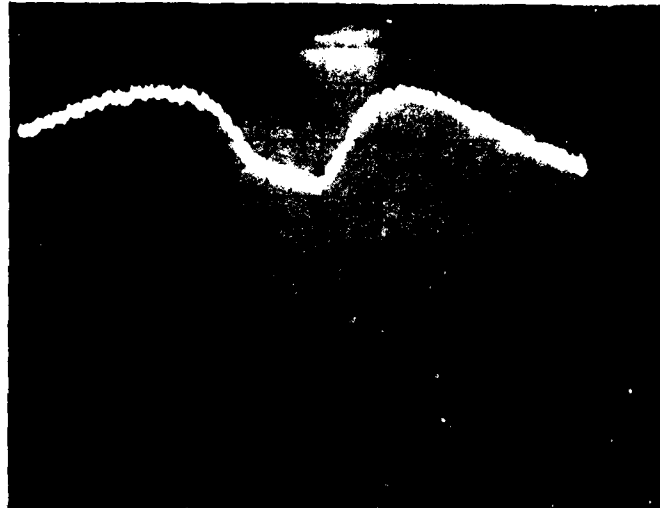


CANCELLED

VERTICAL
SCALE =
10 dB/DIV

CENTER FREQUENCY = 246 MHz
FREQUENCY SPAN = 2 MHz

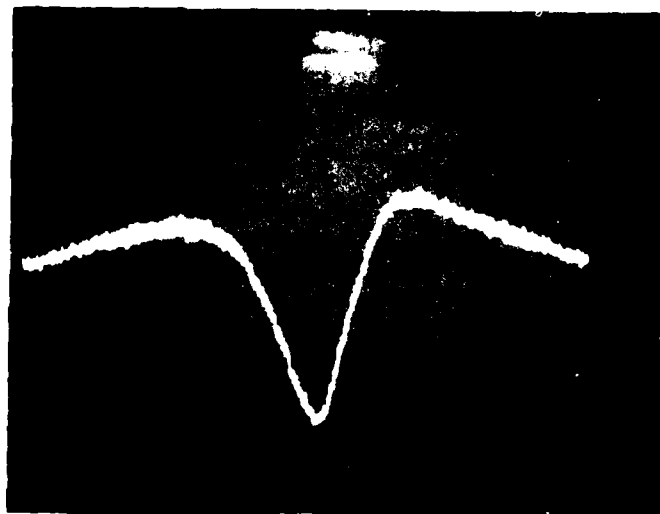
FIGURE 4.16 - AUTOMATIC NONLINEAR CANCELLATION FOR SEPARATE INTERFERING AND REFERENCE NONLINEARITIES EXCITED BY BROADBAND NOTCHED NOISE.



UNCANCELLED

VERTICAL
SCALE =
10 dB/DIV

CENTER FREQUENCY = 246 MHz
FREQUENCY SPAN = 2 MHz



CANCELLED

VERTICAL
SCALE =
10 dB/DIV

CENTER FREQUENCY = 246 MHz
FREQUENCY SPAN = 2 MHz

FIGURE 4.17 - AUTOMATIC NONLINEAR CANCELLATION FOR SINGLE NONLINEARITY

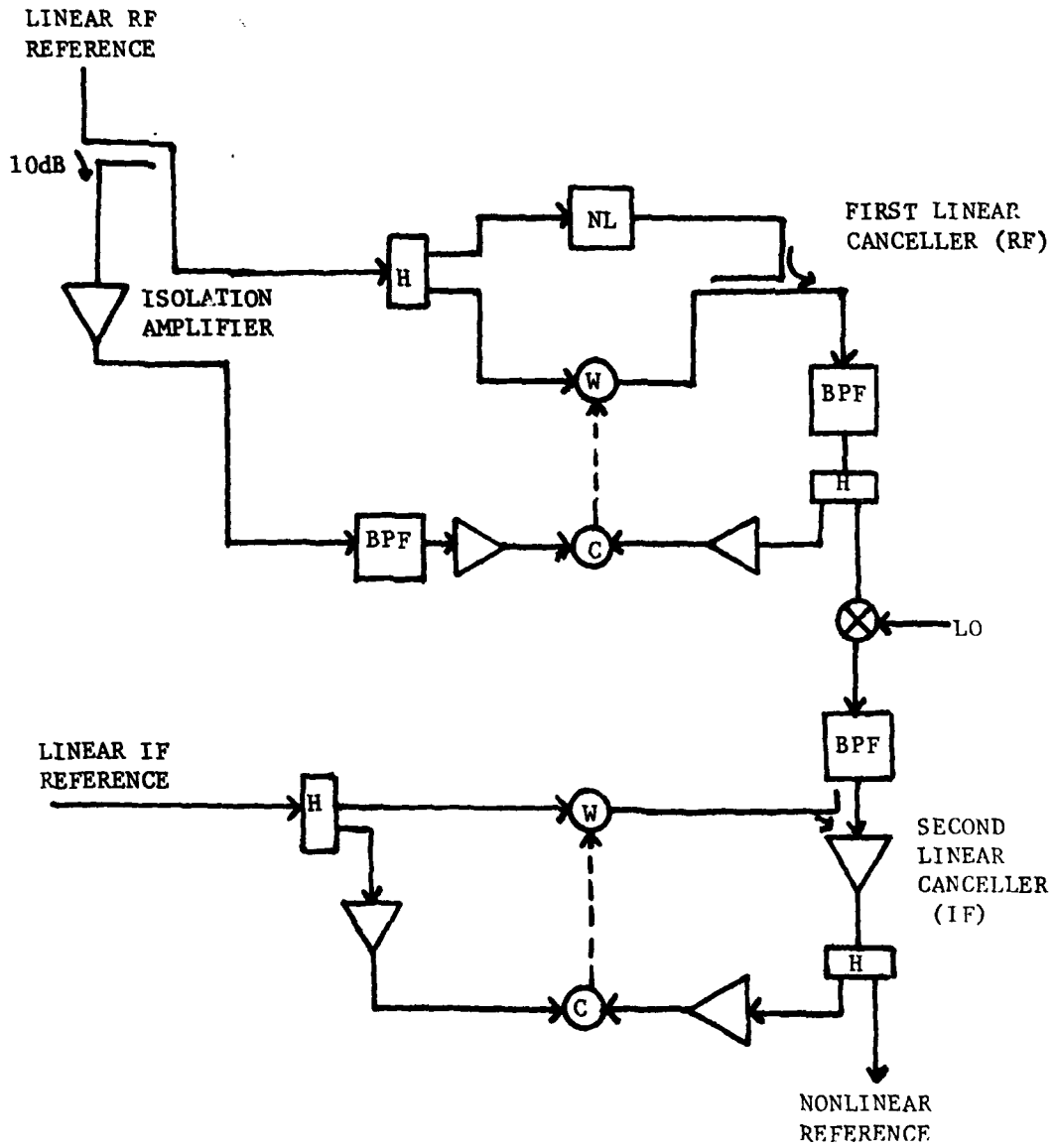


FIGURE 4.18 - AFSATCOM NONLINEAR REFERENCE GENERATOR

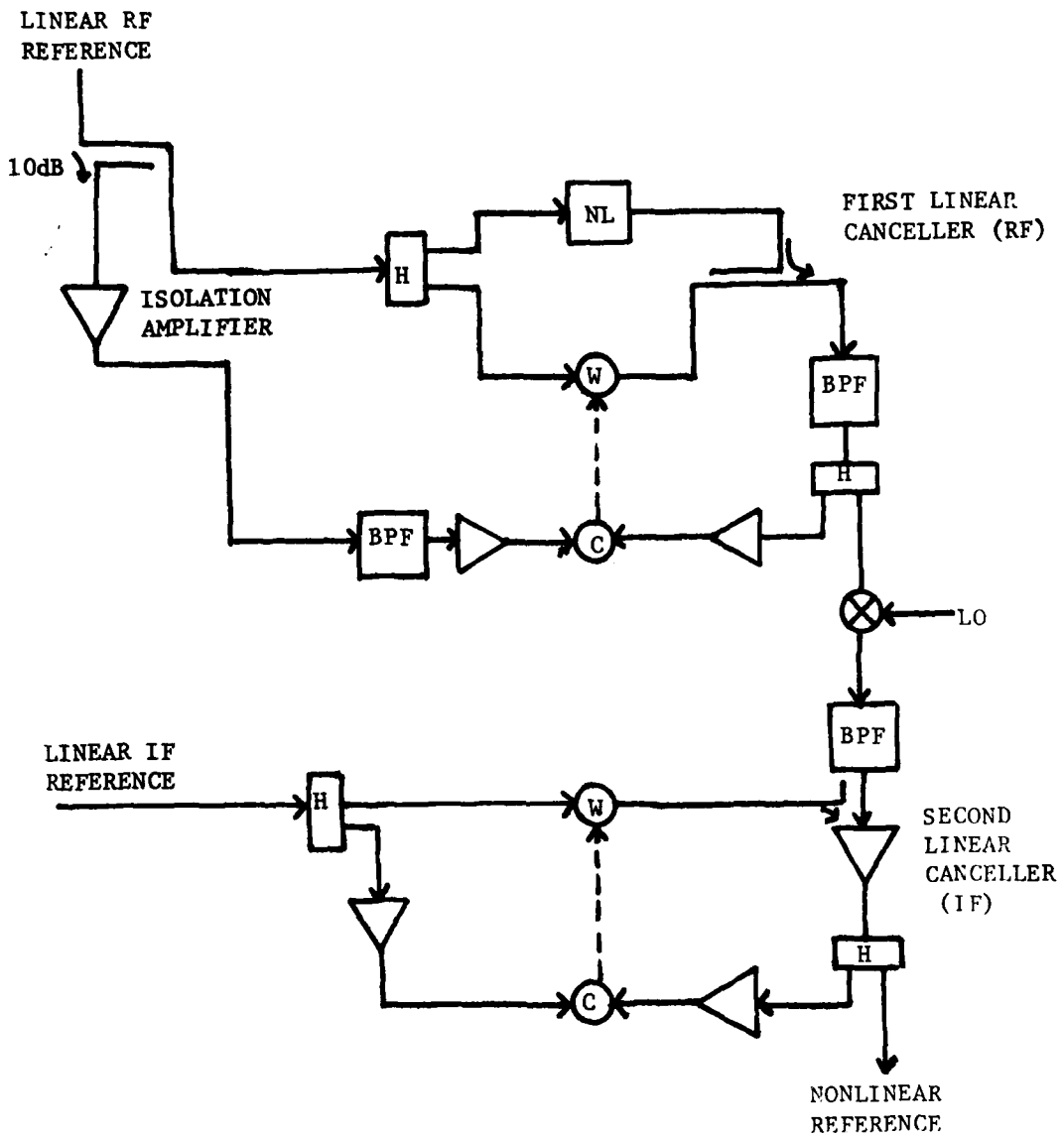
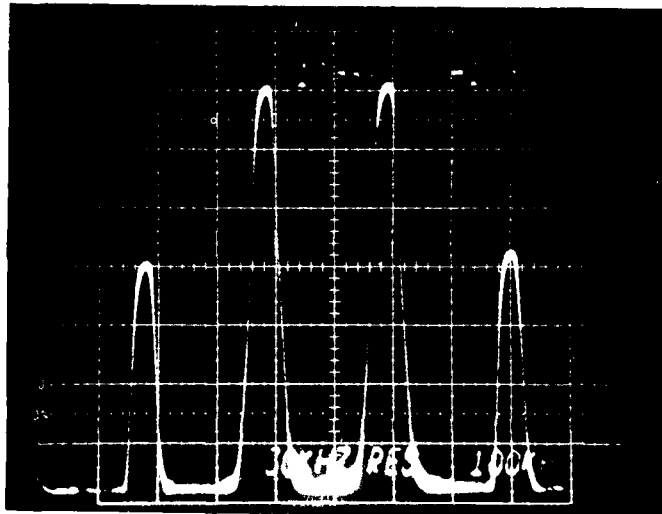


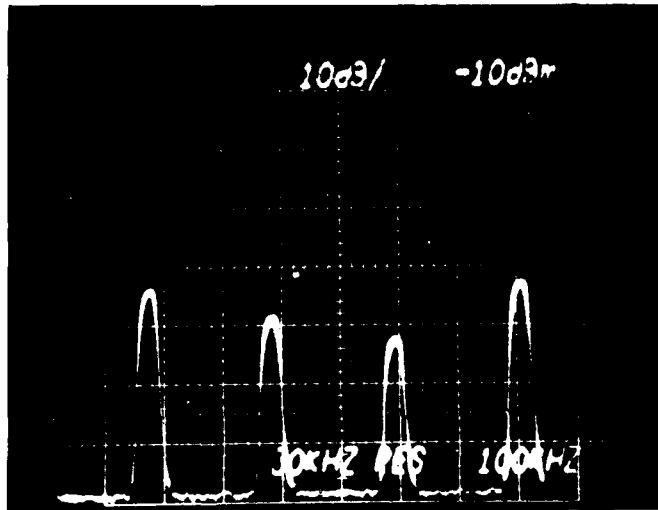
FIGURE 4.18 - AFSATCOM NONLINEAR REFERENCE GENERATOR



\uparrow \uparrow \uparrow \uparrow
 $2f_1 - f_2$ f_1 f_2 $2f_2 - f_1$

UNCANCELLED

REFERENCE:
 NONLIN/LIN
 = -30 dB



\uparrow \uparrow \uparrow \uparrow
 $2f_1 - f_2$ f_1 f_2 $2f_2 - f_1$

CANCELLED

REFERENCE:
 NONLIN/LIN
 = -45 dB

FIGURE 4.19 - OUTPUT OF NONLINEAR REFERENCE GENERATOR FOR TWO-TONE INPUT

generator cancelled and uncanceled. Note that the linear signal components f_1 and f_2 are cancelled below the level of the third-order components $2f_2 - f_1$ and $2f_1 - f_2$.

Figure 4.20 shows the system used to automatically cancel nonlinear interference. In this case, the linear noise in the interfering path was cancelled 80 dB by the AFSATCOM ICS. 10 to 12 dB of nonlinear cancellation was obtained using FH-1100 Schottky diodes as nonlinearities with a 200 MHz incident noise bandwidth.

Use of a nonlinear reference generator has advantages over the notch approach. In many situations, it is impossible to introduce a notch to eliminate the linear signal component. Furthermore, the nonlinear reference generator can operate over a much broader frequency range by simply changing the local oscillator frequency. Disadvantages include the complexity necessary for using an ICS to get a nonlinear reference larger than the linear signal.

A number of experiments were conducted with the AFSATCOM system modified to cancel nonlinearities using the ANLC approach. Cancellation of IMP products by 16 dB was obtained for matched FH-1100 diodes in the interfering and reference paths (Figure 4.21). The system shown in Figure 4.22 was used to investigate the effect of multipath on nonlinear cancellation. In this setup, a straight cable length was inserted in the reference path, while a variable multipath was inserted in the interfering path. As l_1 was increased, nonlinear cancellation degraded from 9 dB at $l_1 = 6$ inches to no cancellation at $l_1 = 19$ feet (Figure 4.23).

Multipath compensation was used to determine if cancellation could be regained. When the compensating reference multipath was made to match the interfering multipath, no degradation of cancellation occurred. Changes in the compensating multipath in the range of ± 2 feet resulted in a complete loss of cancellation.

The system shown in Figure 4.22 was used to test the effect of different nonlinearity types in the interfering and reference paths and no multipath. Table 4.1 shows results obtained for various diode nonlinearities, a saturating amplifier, a detector circuit, and a lowpass nonlinearity. Results indicate that nonlinear cancellation can be achieved with dissimilar types of nonlinearities.

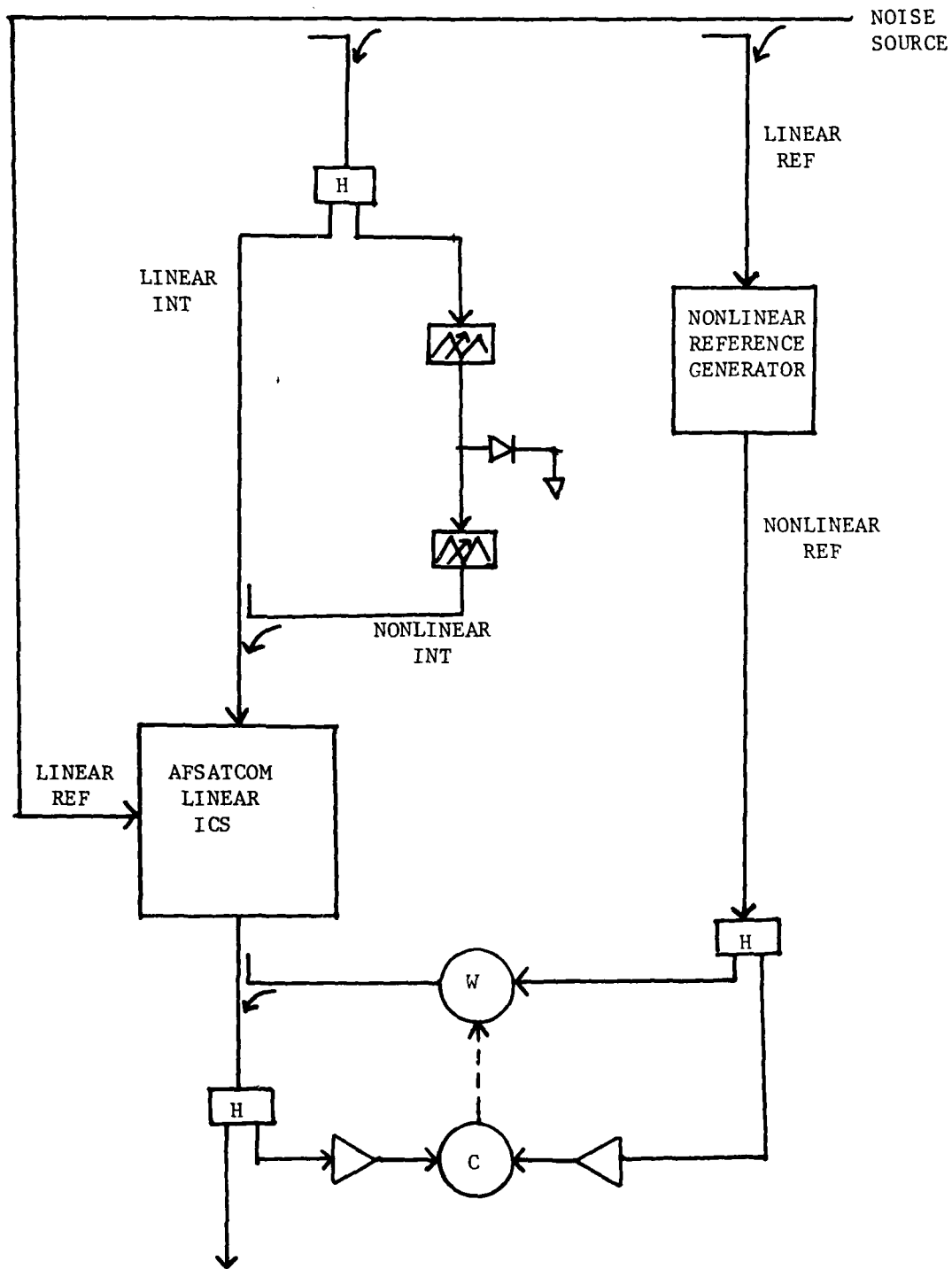


FIGURE 4.20 - SYSTEM USED TO AUTOMATICALLY CANCEL LINEAR AND NONLINEAR INTERFERENCE

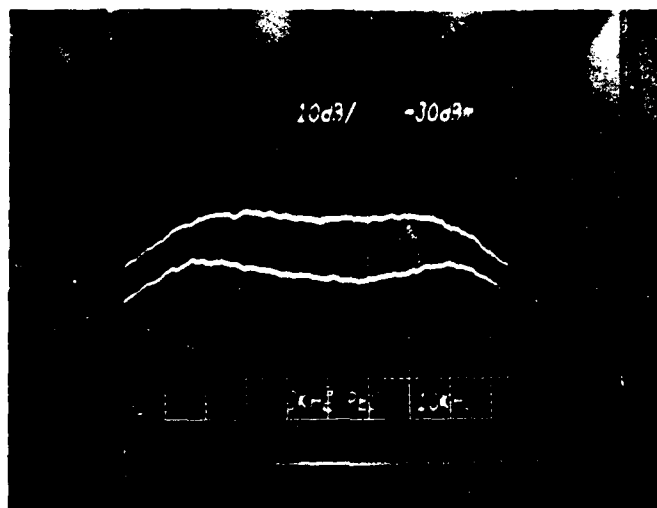


FIGURE 4.21 - CANCELLATION OF IMP'S GENERATED BY MATCHED
EH-1100 DIODES

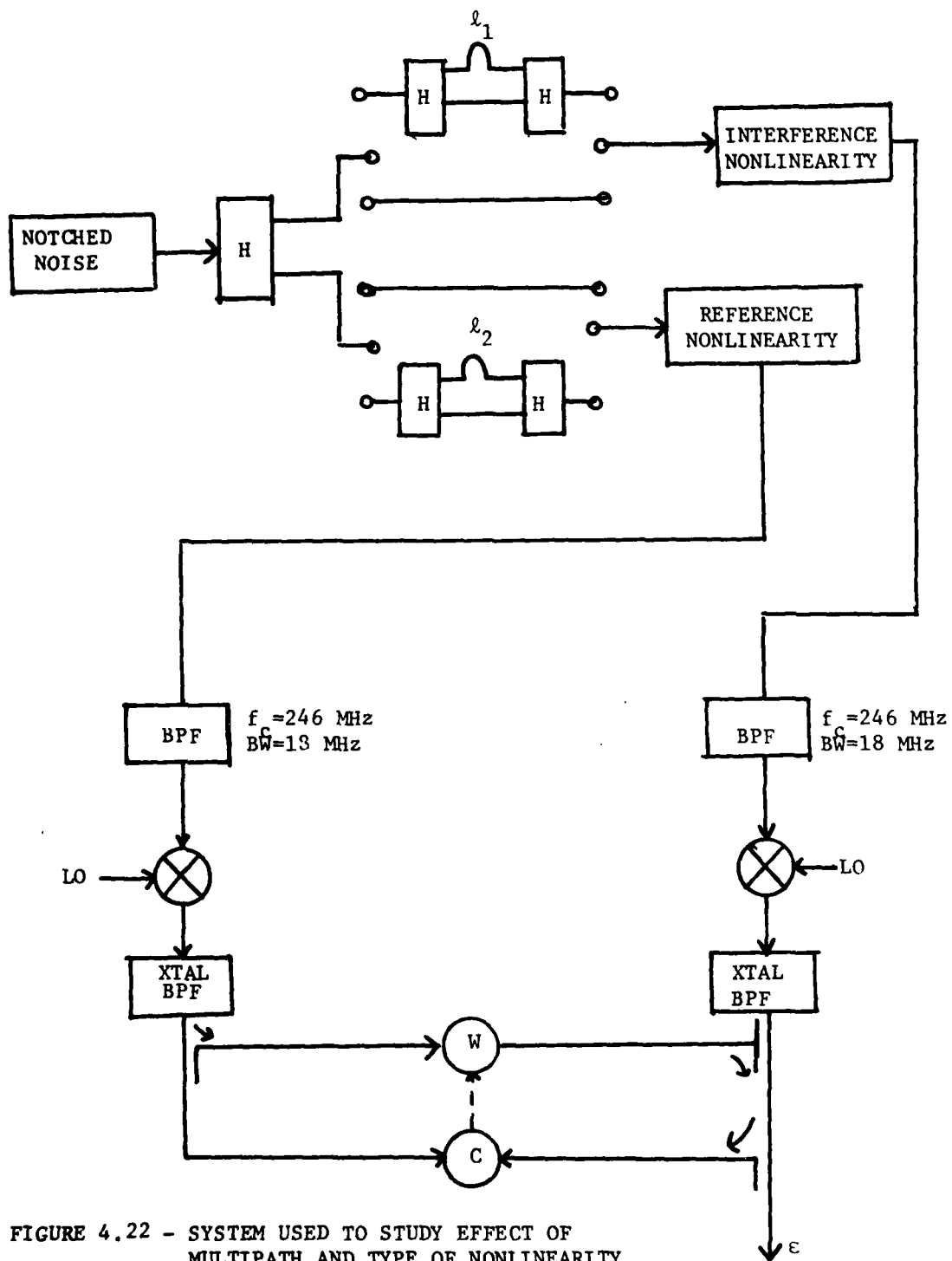
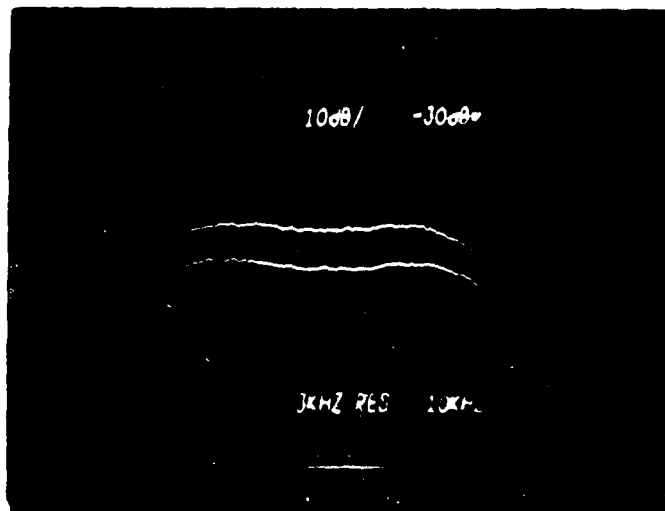
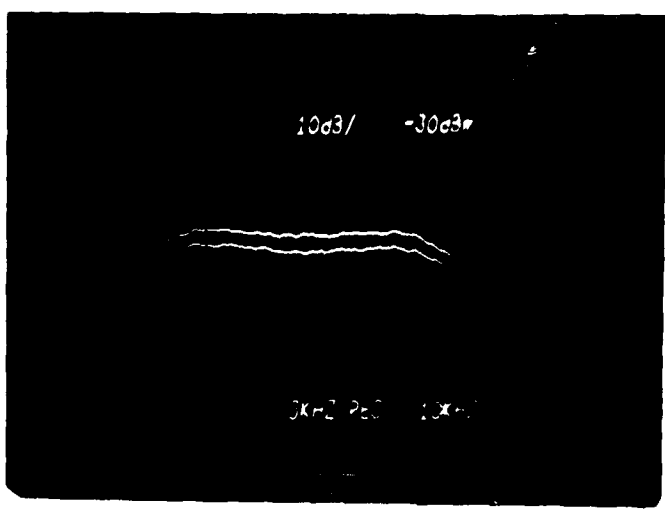


FIGURE 4.22 - SYSTEM USED TO STUDY EFFECT OF MULTIPATH AND TYPE OF NONLINEARITY ON CANCELLATION OF IMPs



$r_1 = 1$ foot



$r_1 = 10$ feet

FIGURE 4.23 - CANCELLATION WITH MULTIPATH IN INTERFERING PATH,
STRAIGHT PATH IN REFERENCE PATH

TABLE 4.1 - CANCELLATION USING DIFFERENT NONLINEAR SOURCES

Reference Nonlinearity	Interference Nonlinearity	Cancellation of IMPs in 100 kHz Bandwidth
FH-1100	FH-1100	16 dB
Detector ⁽¹⁾	Detector	16 dB
Varactor	Detector	8 dB
GPD-403 ⁽²⁾	GPD-403	8 dB
FH-1100	1N939	5 dB
FH-1100	1N4002	4 dB
1N939	GPD-403	3 dB
1N4002	GPD-403	3 dB
Varactor	GPD-403	3 dB
FH-1100	GPD-403	3 dB

(1) The detector consists of a series diode followed by a shunt capacitor and resistor.

(2) The GPD-403 is a broadband amplifier forced into saturation by 0 dBm input noise power in a 200 MHz bandwidth.

5.0 CONCLUSIONS

This study was directed at the analysis and characterization of nonlinearities, and the development of an automatic nonlinear cancellation system. Analysis included the use of power series, Volterra series, and perturbation analysis to predict the generation of intermodulation products. Power series approach was used to predict the effect of bias on IMP generation in a semiconductor diode. Volterra series and perturbation techniques predicted the generation of asymmetric IMPs in systems with memory.

Characterization studies included the use of variable power input two-tone or notch noise to measure IMP generation by various nonlinear devices. Characterization results are necessary to select reference nonlinearities to match the interfering nonlinearity. Bias on a diode can be used to achieve a "hard" or "soft" nonlinearity, or to obtain asymmetric IMPs.

Manual and automatic nonlinear interference cancellation systems were designed and implemented. Experimental studies were conducted using different nonlinearities, a wide range of input powers, a wide range of frequency spectra exciting the nonlinearities, various delays and multipath before and after the nonlinearities, and a number of modulation formats. Based on these experimental studies, a list of necessary conditions for nonlinear cancellation were developed. To achieve good automatic nonlinear cancellation, the following conditions must be met:

1) A good nonlinear reference must be generated. This can be achieved by using either an ICS to cancel or a notch filter to reduce the linear signal component below the nonlinear component.

2) Amplitude vs frequency shape of the signal impinging on the interfering and reference nonlinearities are critically important for good nonlinear cancellation. This is because distortion contribution coming from intermodulation products are generated from frequency components over the entire noise bandwidth.

3) Interfering and reference nonlinearity types must be matched. This is because different nonlinearities may contribute different intermodulation products from an identical excitation.

4) Multipath before the interfering and reference nonlinearities is critically important. A multipath difference on the order of a few feet will cause complete loss of cancellation.

5) The total power input to the reference nonlinearity must be similar to that of the interfering nonlinearity for good cancellation.

A number of conditions have been found not to be important in achieving good nonlinear cancellation. Among these are:

1) Certain types of phase vs frequency variation in the signal impinging on the reference or interference nonlinearity does not affect cancellation. For example, FM experiments and insertion of various delays before the interfering nonlinearity had no effect on cancellation.

2) Multipath or bulk delay following the nonlinearity does not affect cancellation. This is because only narrowband cancellation after the nonlinearity (approximately 100 kHz) was examined.

5.1 RECOMMENDATIONS

A large gap remains to be bridged between the use of an experimental laboratory nonlinear interference cancellation system to cancel IMPs generated by diodes to a system capable of cancelling IMPs generated on aircraft. A number of steps need to be taken to help bridge this gap. Further analysis can be conducted using the Volterra approach to analyze more complicated and realistic systems. Use of NCAP and IMOD programs from RADC/RBCTI would be needed to assist in the analysis. Cancellation could next be attempted using actual communication equipment as a source of nonlinear interference (Figure 5.1). After cancellation is achieved using a cable path, the system could be set up in an anechoic chamber (Figure 5.2). If this is successful, cancellation could then be attempted aboard an aircraft.

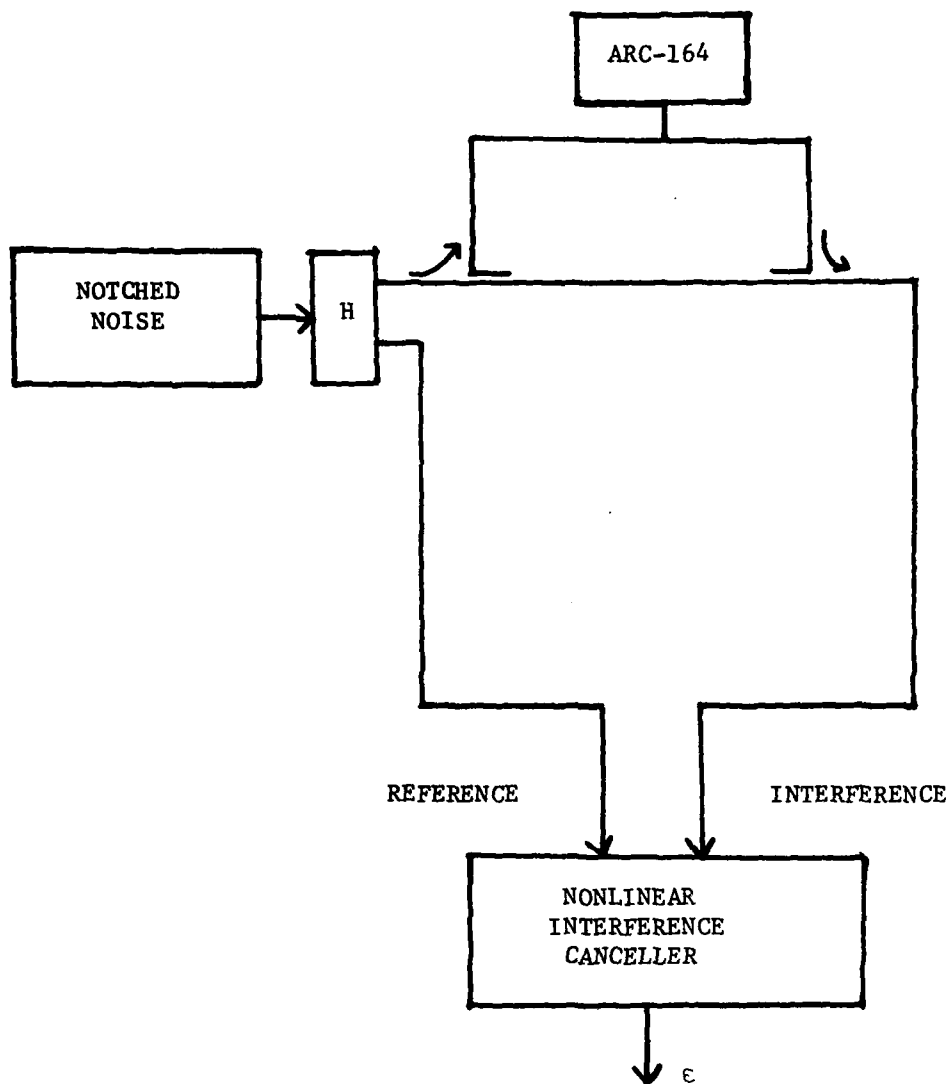


FIGURE 5.1 - CANCELLATION OF IMPs GENERATED BY ARC-164

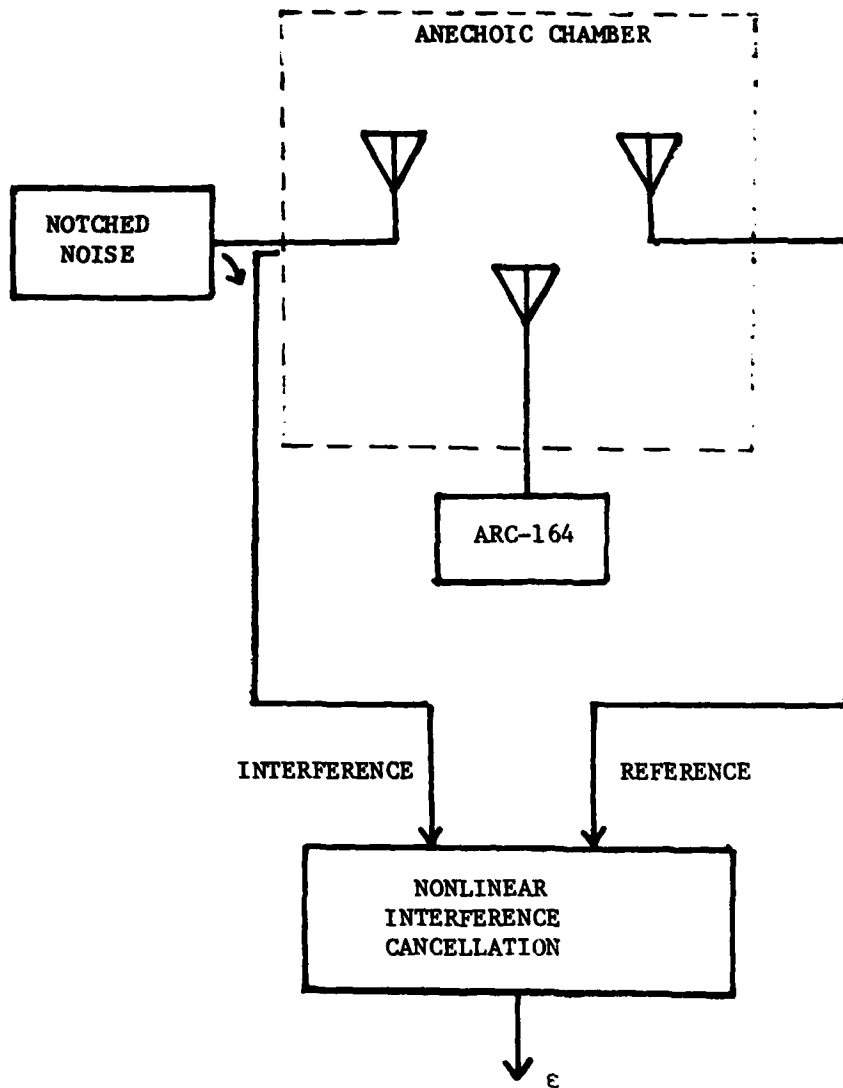


FIGURE 5.2 - CANCELLATION OF IMPs GENERATED BY ARC-164 IN ANECHOIC CHAMBER

APPENDIX A

NOISE THROUGH A THIRD-ORDER NONLINEARITY

$$\text{Let } y(t) = \alpha x^3(t)$$

where α is in volts⁻².

$$R_y(\tau) = 9\alpha^2 \sigma^4 R_x(\tau) + 6\alpha^2 R_x^3(\tau)$$

If $S_x(f) = A$ for $|f| < B/2$,

where $A = \text{volts}^2/\text{Hz}$

$B = \text{noise bandwidth}$

then

$$R_x^3(\tau) \leftrightarrow S_x(f) * S_x(f) * S_x(f)$$

Convolving graphically as shown in Figure A-1:

$$S_x(f) * S_x(f) = A^2 B \left(1 - \frac{|f|}{B}\right)$$

Graphically convolving $S_x(f)$ with $S_x(f) * S_x(f)$ as shown in Figure A-1,

$$S_x(f) * S_x(f) * S_x(f) = \begin{cases} \frac{A^3 B^2}{2} \left(\frac{3}{2} + \frac{f}{B}\right)^2 & \text{for } -\frac{3B}{2} < f < -\frac{B}{2} \\ A^3 B^2 \left(\frac{3}{4} - \frac{f^2}{B^2}\right) & \text{for } -\frac{B}{2} < f < \frac{B}{2} \\ \frac{A^3 B^2}{2} \left(\frac{3}{2} - \frac{f}{B}\right)^2 & \text{for } \frac{B}{2} < f < \frac{3B}{2} \end{cases}$$

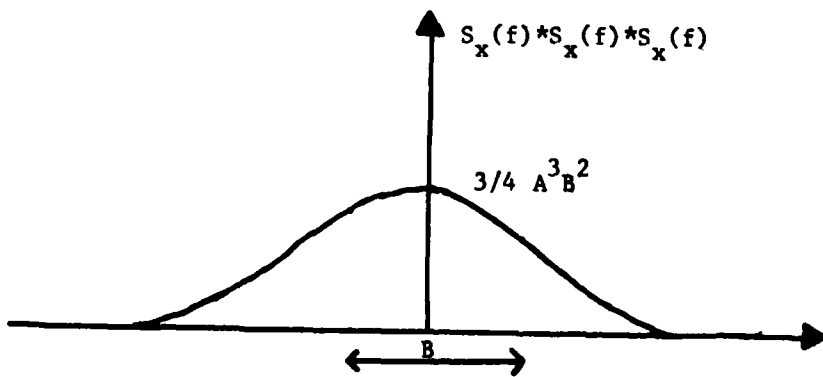
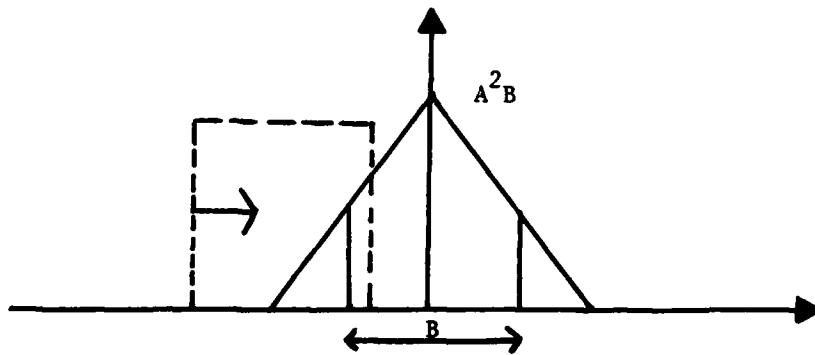
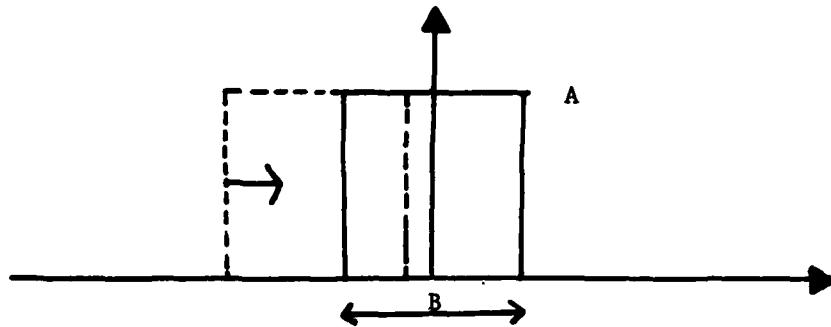


FIGURE A-1. GRAPHICAL CONVOLUTION TO OBTAIN $S_x(f) * S_x(f) * S_x(f)$

REFERENCES

- [1] "Nonlinear Interference Cancellation System," RADC-TR-78-225, November 1978. (B032512L)
- [2] Higa, Walter H. "Spurious Signals Generated by Electron Tunneling on Large Reflector Antennas," Proc IEEE, vol. 63, no. 2, February 1975.
- [3] Chase W.M. J.W. Rockway and G.C. Salisbury "A Method of Detecting Significant Sources of Intermodulation Interference," IEEE Trans on Electromagnetic Compatibility, vol. EMC-17, no. 2, May 1975.
- [4] Chase, W.M., "Ship RFI Survey Procedure for HF Frequencies," NELC Technical Document 336, 21 June 1974.
- [5] Bond, C.D., Guenzer, C.S., "Intermodulation Generation by Electron Tunneling Through Aluminum-Oxide Film," Proc IEEE, vol. 67, no. 12, December 1979.
- [6] Arazm, F., Benson, F.A., "Nonlinearities in Metal Contacts at Microwave Frequencies," IEEE Trans on Electromagnetic Compatibility, vol. EMC-22, no. 3, August 1980.
- [7] Lee, J.C., "Intermodulation Measurement in the UHF Band and an Analysis of Some Basic Materials," Lincoln Laboratory Technical Note 1979.
- [8] Wiener, N., Nonlinear Problems in Random Theory, MIT Press, 1958.
- [9] "Nonlinearity System Modelling and Analysis with Application to Communication Receivers," RADC-TR-73-178, June 1973. (766278)
- [10] Spina, J.E., Weiner D.D., Sinusoidal Analysis of Weakly Nonlinear Circuits, Van Nostrand Reinhold Co., 1980
- [11] Schetzen, M , The Volterra and Wiener Theories of Nonlinear Systems, John Wiley and Sons, New York, 1980.
- [12] Colemeier, J., "Air Force Electromagnetic Compatibility Intrasystem Analysis Program," RADC, 1980.
- [13] Gretsch, W.R., "The Spectrum of Intermodulation Generated in a Semiconductor Diode Junction," Proc IEEE, vol. 54, no. 11, November 1966.
- [14] Lotsch, H.K., "Theory of Nonlinear Distortion Produced in a Semiconductor Diode," IEEE Trans on Electron Devices, vol. ED-15, no. 5 May 1968.

- [15] Bava, E., et al, "Analysis of Varactor Frequency Multiplexers: Nonlinear Behavior and Hysteresis Phenomena," IEEE Trans on Military Technology, vol. 27, no. 2, February 1979.
- [16] "Intermodulation in Antenna Amplifiers," Amperex Application Report S-141, 1980.
- [17] Falconer D.D., "Adaptive Equalization of Channel Nonlinearities in QAM Data Transmission Systems," BSIJ, vol. 57, no. 7, September 1978.



MISSION
of
Rome Air Development Center

RADC plans and executes research, development, test and selected acquisition programs in support of Command, Control Communications and Intelligence (C³I) activities. Technical and engineering support within areas of technical competence is provided to ESD Program Offices (POs) and other ESD elements. The principal technical mission areas are communications, electromagnetic guidance and control, surveillance of ground and aerospace objects, intelligence data collection and handling, information system technology, ionospheric propagation, solid state sciences, microwave physics and electronic reliability, maintainability and compatibility.